LAPPEENRANTA UNIVERSITY OF TECHNOLOGY
Faculty of Technology
Master's Degree Program in Energy Technology

Teemu Sihvonen

Dynamic carbon dioxide liquidization model

Examiners: Professor Timo Hyppänen
Associate Professor Tero Tynjälä
Supervisor: M.Sc. Matti Tähtinen

Lappeenranta, April 22, 2015

ABSTRACT

Lappeenranta University of Technology
Faculty of Technology
Master's Degree Program in Energy Technology

Teemu Sihvonen

Dynamic carbon dioxide liquidization model

Master's thesis

2015

67 pages, 27 figures and 12 tables

Examiners: Professor Timo Hyppänen
Associate Professor Tero Tynjälä

Keywords: Apros, CO_2 liquidization, dynamic model

In literature CO_2 liquidization is well studied with steady state modeling. Steady state modeling gives an overview of the process but it doesn't give information about process behavior during transients. In this master's thesis three dynamic models of CO_2 liquidization were made and tested. Models were straight multi-stage compression model and two compression liquid pumping models, one with and one without cold energy recovery. Models were made with Apros software, models were also used to verify that Apros is capable to model phase changes and over critical state of CO_2. Models were verified against compressor manufacturer's data and simulation results presented in literature. From the models made in this thesis, straight compression model was found to be the most energy efficient and fastest to react to transients. Also Apros was found to be capable tool for dynamic liquidization modeling.

TIIVISTELMÄ

Lappeenrannan teknillinen yliopisto
Teknillinen tiedekunta
Energiatekniikka

Teemu Sihvonen

Dynaaminen hiilidioksidin nesteyttämismalli

Diplomityö

2015

67 sivua, 27 kuvaa ja 12 taulukkoa

Tarkastajat: Professori Timo Hyppänen
Tutkijaopettaja Tero Tynjälä

Hakusanat: Apros, CO_2 nesteyttäminen, dynaaminen malli

Kirjallisuudessa hiilidioksidin nesteyttämistä on tutkittu paljon stationäärisellä mallintamisella. Stationääriset mallit antavat yleiskuvan prosessista, mutta niillä ei saada tietoa prosessin käyttäytymisestä muutosten aikan. Tässä diplomityössä tehtiin kolme dynaamista mallia hiilidioksidin nesteytyksestä. Mallit olivat suora monivaiheinen kompressio ja kaksi kompressio-nesteen pumppausmallia, joista toisessa oli ja toisessa ei ollut kylmäenergian talteenottoa. Mallit tehtiin Apros ohjelmistolla ja malleja käytettiin myös varmistamaan, että Apros kykenee mallintamaan CO_2:sen faasimuutokset ja ylikriittisen tilan. Mallien toiminta todennettiin kompressorivalmistajan mittausarvoilla ja kirjallisuudessa esitetyillä simulointituloksilla. Tässä työssä esitetyistä malleista suorakompressiomalli todettiin kaikkein energiatehokkaimmaksi ja nopeimmaksi muutostilanteissa. Lisäksi Apros todettiin toimivaksi työkaluksi nesteyttämisen dynaamiseen mallinukseen.

CONTENTS

NOMENCLATURE

Abbreviations

ASU	air separation unit
ATR	auto–thermal reforming
AZEP	advanced zero emission process
CC	combined cycle
CCS	carbon capture and storage
CLC	chemical looping combustion
CPU	CO2 processing unit
ECBM	enhanced coal bed methane
EGR	enhanced gas recovery
EOR	enhanced oil recovery
GHG	green house gas
GT	gas turbine
HP	high pressure
IGCC	integrated gasification combined cycle
LNG	liquefied natural gas
LP	low pressure
MSR–H2	methane steam reformer with hydrogen separation
ppm	parts per million
ppmbw	ppm by weight
S–Graz	high steam content Graz cycle
SOFC	solid oxide fuel cell
WC	water cycle
VTT	Technical research center of Finland

Roman symbols

c	speed of sound	m/s
c_p	isobaric specific heat capacity	J/kgK
c_v	isochoric specific heat capacity	J/kgK
k	ratio of specific heats, $\frac{cp}{cv}$	-
F	molar flow rate	mol/s
M	molar weight	kg/mol

N	number of carbon atoms	
P	power	W
p	pressure	Pa
q_m	mass flow	kg/s
R	specific gas constant, $\frac{R_u}{M}$	J/kgK
R_u	universal gas constant	J/molK
S	selectivity	%
SM	surge margin	%
T	temperature	K
V_m	molar volume	m^3/mol
X	conversion	%
Y	yield	%

Greek symbols

η_p	polytropic efficiency	-

Subscripts

1	inlet
2	outlet
comp	compressor
i	product or species
ideal	ideal gas
in	inlet
out	outlet
s	surge point
w	operating point

1 INTRODUCTION

1.1 Background

Global warming is one of the great concerns of this century. Global warming is caused largely by greenhouse gas (GHG) emissions, especially carbon dioxide (CO_2) (Xu et al., 2014). In figure 1 is presented percentage distribution of main greenhouse gases globally in year 2004 IPCC (2007). As can be seen from figure 1 CO_2 is largest component of anthropogenic GHG.

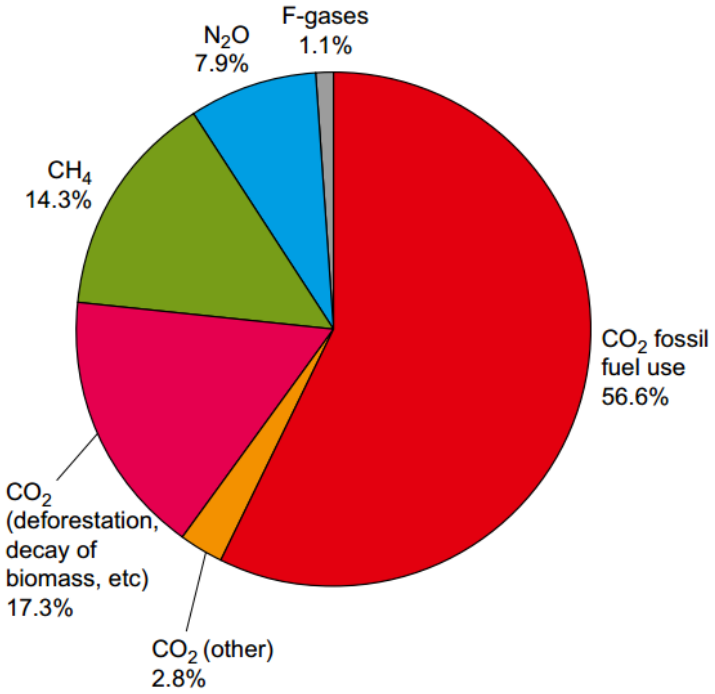

Figure 1: Percentage distribution of man made greenhouse gas emissions in 2004. IPCC (2007)

To reduce CO_2 emissions there are couple of different approaches: improving efficiency, switching to less carbon-intensive fuels, nuclear power, renewable energy sources and carbon dioxide capture and storage (CCS) (IPCC, 2005). From these possibilities only CCS can generate step-change that is needed at the moment (Wall, 2007). CCS technologies allow capturing and transporting CO_2 emissions from large point sources to safe storage or usage sites, rather than being emitted to atmosphere (Gibbins and Chalmers, 2008). In current energy infrastructure fossil fuel fired power plants are these large point sources of CO_2 emissions (figure

1). CCS would give fossil fuel power plants possibility to sustain their operations for longer time, until alternative energy sources can replace them or they can meet the strict environmental regulations (Zanganeh and Shafeen, 2007).

Fu and Gundersen (2012) states, based on (IEA, 2007), that CCS reduces power plants efficiency 9 and 6 percentage for coal fired power plants and natural gas power plant respectively when an amine-based post-combustion capture system is applied. For Integrated Gasification Combined Cycle (IGCC) plant with pre-combustion CO_2 capture the efficiency lost is around 8.5 percentage points. At oxy-combustion process the combustion is oxidized with oxygen instead of air and thus the flue gas is mainly CO_2 and H_2O. From there CO_2 can be separated simply by condensing the H_2O. The air separation unit (ASU) and the CO_2 compression and purification unit (CPU) causes 6.5 and 3.5 percentage point reduction to plant efficiency respectively. The total efficiency penalty can be reduced to 8 percentage points by heat integration between the ASU and CPU. (Fu and Gundersen, 2012) 2nd generation CO_2 capture technologies, that should be in use by 2030, are predicted to be 30 % more energy efficient than the 1st generation technologies used at the moment (CSLF, 2013).

For all of the capture technologies compression of CO_2 is one of the main penalty causer (Fu and Gundersen, 2012). For coal fired power plant CO_2 liquefaction efficiency penalty is from 3 to 4 percentage points and for natural gas based power plants about 2 percentage points (Göttlicher, 2004). Compression equipments are around 25% of the total capital requirements for CCS process and compression causes additional 3.5 €/MWh to cost of electricity (Romeo et al., 2009). There is a great need to understand the existing technologies to improve the performance and to reduce the cost and energy requirements for carbon dioxide compression.

Modeling makes it possible to study methods to reduce the energy consumption of CO_2 liquidization process without construction of expensive test facilities. Steady state and full time operation has been the focus for many studies, while the optimization of process during dynamic operation is often overlooked. With dynamic simulations it is possible to understand the dynamics of the process for example during shut downs and startups. From literature can be found many steady state model studies for the CO_2 compression process (Alabdulkarem et al., 2012, Am-

rollahi et al., 2011, Cifre et al., 2009, Möller et al., 2007, Pfaff et al., 2010, Romeo et al., 2009, Sanpasertparnich et al., 2010). Full time continuous CO_2 capture might not be economically feasible, thus dynamic operation must be considered (Bui et al., 2014). While capture process might not be continuous, the liquidization process need to follow it dynamically.

1.2 Objective

Objective of this thesis is to understand CO_2 liquidization process and to make dynamic model of it for VTT's use. Model is made with Apros 6 Combustion dynamic process simulation software. Apros has high accuracy for processes where water or water steam is the working fluid. CO_2 liquidization model is also used to check that Apros can handle phase changes and over critical states of other fluids than water as well.

1.3 Structure of the thesis

Structure of the thesis is divided into two main parts, literature and experimental parts. Literature part consists sections 2 to 4 and experimental part is presented in sections 5 and 6.

Firstly literature part presents CO_2 liquidization process in thermodynamic sense in section 2. What needs to be done for the CO_2 during the liquidization process and what kind of equipments are used in the process are also presented in this section. Section 3 consists CO_2 transportation methods, and section 4 presents some storage and utilization methods for CO_2. Main focus in sections 3 and 4 is on pressure and temperature levels for these processes, as these are important to know in liquidization process.

Experimental part gives an overview of Apros modeling software and liquidization models made with it in section 5. Example simulations and results are presented in section 6. Lastly in section 7 is conclusions of the thesis.

2 LIQUIDIZATION PROCESS

CO_2 emissions from fossil fuels and cement production companied were 36 Gt in year 2013 (Le Quéré et al., 2014). Ideally almost all of these emissions are captured and transported to safe storage or to usage sites. Geological storages, enhanced oil recovery, unmineable coal bed or storage in saline aquifers, are currently thought as safe storages. Carbon dioxide can also be used in industry (food beverages, refrigerant), agriculture (making ammonia and urea) or energy production (methanation). (Leung et al., 2014) More about storing and utilization in section 4. To make this transportation as energy efficiently as possible CO_2 needs to be liquidized (Aspelund et al., 2006, IPCC, 2005). Carbon dioxide is either compressed and cooled to liquid state or to supercritical state, depending on how it is transported onwards from the compression site. Basically in ships CO_2 is transported in liquid state (Aspelund et al., 2006) and as supercritical fluid in pipeline (Aspelund and Jordal, 2007, IPCC, 2005). More accurately about transportation in section 3.

For liquidization carbon dioxide needs to be compressed or compressed and cooled until it reaches liquid or supercritical state. In figure 2 on the upper diagram is shown carbon dioxides phase diagram in respect to temperature and pressure. Lower diagram in figure 2 presents density of carbon dioxide in respect to pressure and temperature, dashed line is the border of supercritical region (Friedmann, 2007). Diagrams are for pure CO_2. In their study Chapoy et al. (2013) got results that impurities (5.05% O_2, 2.05% Ar, 3.07% N_2) in CO_2 stream changes the critical point to be at 23.8 °C and 87.9 bar. Density of impure CO_2 stream is from $180\,\mathrm{kg\,m^{-3}}$ (at 120 bar) to $50\,\mathrm{kg\,m^{-3}}$ (>120 bar) lower than for pure CO_2 (Chapoy et al., 2013). To improve energy efficiency of compression and transportation it's crucial to reach as pure stream of CO_2 as possible while keeping in mind both energy and capital costs of purification (Aspelund and Jordal, 2007).

Two theoretical liquidization paths for CO_2 are isothermal and isentropic paths. These paths for from 1 to 140 bar pressurizing are presented in figure 3. On isothermal path temperature of CO_2 is not changing as pressure is increasing and on isentropic path entropy stays constant. It is possible to achieve near isentropic liquidization process with high efficiency compressors, but on isentropic liquidization CO_2 heats up significantly if

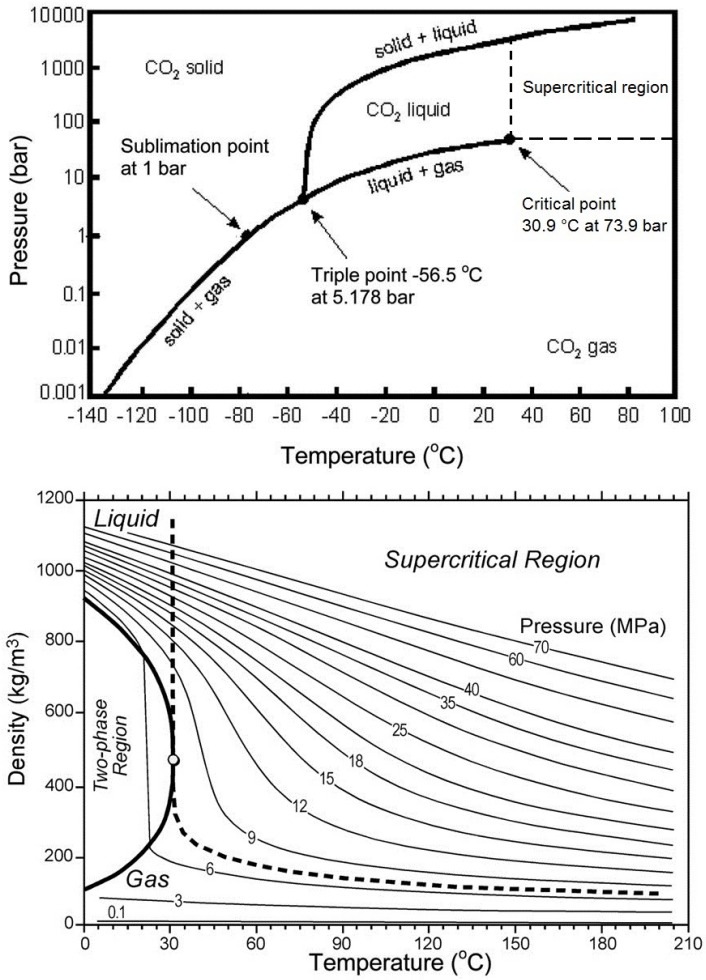

Figure 2: Carbon dioxide phase (upper) and density (lower) diagrams in respect to pressure and temperature. (Friedmann, 2007)

pressurized up to 140 bar pressure. As already shown in figure 2, CO_2 temperature should be kept as low as possible, to achieve highest density. With isentopic liquidization this is not possible. Thus more sensible path for liquidization is isothermal path. Later in figure 7 it's shown how is possible to achieve close to isothermal liquidization process.

2.1 Removal of impurities

Capture methods don't provide pure CO_2 stream. In this theses capture processes are not presented, but good overviews of these processes are provided by Kvamsdal et al. (2007) and by Leung et al. (2014). In table 2 are quality levels of captured gas from different capture processes with pressure and temperature levels. These impurities need to be removed

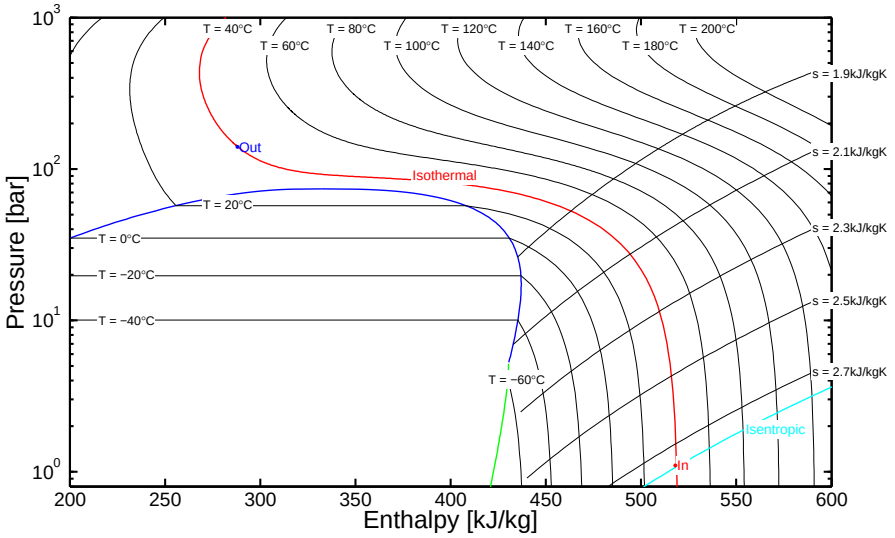

Figure 3: Comparison of isothermal (red line) and start of isentropic (green line) liquidization paths from 1 bar (In) to 140 bars (Out), inlet and outlet are at 40 °C temperature. Blue line is vapor dome.

from CO_2 stream because of requirements of transportation methods, also storing method effect on purity level required (Aspelund and Jordal, 2007). More about purity requirements in sections 3 and 4.

Table 2: Gas components (mol-%), pressure and temperature for captured gas from the various capture processes for natural gas fired power plant with sulphur free fuel. (Aspelund and Jordal, 2007)

	CO_2	H_2O	H_2	CO	N_2	O_2	CH_4	Ar	P (bar)	T (°C)
Amine (post-combustion)	94.39	5.61	0	0	0	Traces	0	0	1.01	35
ATR (pre-combustion with amine)	98.21	1.79	0	0	0	0	0	0	1.01	16
Water cycle (WC)	59.74	32.84	0	0.01	2.81	1	0	3.59	0.045	13
S-Graz	61.65	30.90	0	0	2.91	0.85	0	3.69	1.01	337
Oxyfuel CC	93.82	4.16	0	0	0.28	1.38	0	0.35	1.01	30
SOFC + GT	35.90	63.84	0	0	0.26	0	0	0	1.01	439
AZEP HP	35.90	63.84	0	0	0.26	0	0	0	15.38	248
AZEP LP	35.90	63.84	0	0	0.26	0	0	0	1.01	111
CLC	34.66	65.06	0	0	0.28	0	0	0	1.01	415
MSR-H2 HP	62.44	35.49	0.92	0.57	0.45	0	0.12	0	63.94	578
MSR-H2 LP	62.44	35.49	0.92	0.57	0.45	0	0.12	0	1.04	98

In his master's thesis Bilsbak (2009) has composition levels of CO_2 stream for different capture methods. These results are for natural gas and for coal fired power plants. Results are otherwise similar to ones given by Aspelund and Jordal (2007), but Bilsbak (2009) state that there are also some traces of SO_2 and NO in the captured flue gases of oxy fuel natural gas fired power plant. Levels are around 0.014% for both components.

And for coal fired power plant there are some levels of H_2S, SOx and NOx in captured gas stream depending on the method used (Bilsbak, 2009).

As can be seen from table 2, largest impurity in CO_2 stream is water. Water must be removed to avoid gas hydrates, freezing of water and corrosion. Vapor-liquid separation drums are used before the compression to make sure that no liquid is entering to compressors. As solubility of water in CO_2 gas decreases with higher pressures and lower temperatures, it is possible to get water to 400–500 ppm level at pressure between 20 and 40 bar. With adsorption drier CO_2 can be dried to one digit ppm level. These adsorption columns need to be regenerated by heat which increases energy consumption of the drying proses. At this point contaminants like H_2S can also be removed. (Aspelund and Jordal, 2007)

Removed water includes some amount of dissolved CO_2. If this water is not treated CO_2 will be lost to ambient. Especially on processes that contain large amounts of CO_2 contained waters, it should be considered to make CO_2 capture process so that CO_2 emissions in water are kept low. Carbon dioxide increases acidity in water. At low pressure and high temperature levels CO_2 solubility to water is low. Thus by lowering the pressure of removed water dissolved CO_2 can be removed and recaptured. (Aspelund and Jordal, 2007) Adsorption sieve that removes H_2S adsorbs also CO_2. Adsorption for H_2S is stronger than for CO_2 and thus it is possible to do selective H_2S removing from the gas stream. With adsorption H_2S can reach levels less than 0.96 ppm. (Kohl and Nielsen, 1997a)

Removal of hydrogen and carbon monoxide can be done by a combustion reaction, either thermal or catalytic. Combustion needs oxidant, either pure oxygen or air. Thermal combustion needs temperature close to 650 °C and catalytic around 320 °C temperature. This means that for thermal combustion it is almost certain that additional fuel is needed even though combustion reactions develop heat. If the combustion is complete will oxidation of hydrogen and carbon monoxide product only water and carbon dioxide, which is not a problem. (Bilsbak, 2009)

There are two ways to remove volatiles (N_2, Ar, O_2, NO, H_2, CH_4 and CO) from CO_2 gas stream. First is two stage flashing, where dried and compressed CO_2 stream is expanded and thus cooled. Cooled CO_2 will

turn to liquid while volatiles with lower liquidization point will stay in gas phase. Aspelund and Jordal (2007) mention that this method should not be used because all of the CO_2 is not removing from the volatile purge stream. Second method is distillation column, where CO_2 is condensed in a distillation column while volatiles stay in gas phase. Liquid CO_2 is removed from the bottom of the column while volatile purge stream is removed from the top. On the top of the column is condenser where volatile purge gas is partly condensed to capture CO_2 that might otherwise leave with volatiles. And on the bottom of distillation column is a re-boiler that removes volatiles in CO_2 liquid. (Bilsbak, 2009)

Sulphur dioxide (SO_2) is removed either by wet lime scrubbing or by ammonium sulphat process. Precise descriptions about these processes can be found from paper by Kohl and Nielsen (1997b). SO_2 can't be removed by flashing or by distillation column, like other volatiles, because it has boiling point similar to CO_2. (Aspelund and Jordal, 2007)

2.2 CO_2 compressors

Compressors used in CO_2 liquidization process are multi stage centrifugal compressors (Alabdulkarem et al., 2012, Aspelund and Jordal, 2007). In figure 4 is shown a multi stage centrifugal compressor (Asia Vacuum Pumps, 2015). The reason that CO_2 compression in CCS projects is expensive is firstly because the overall pressure ratio is about 100:1 for the process. Second reason is that CO_2 compressors need to be manufactured from stainless steel to prevent corrosion from water vapor. Third and most significant reason is that pressure ratio for one compression stage is limited by aerodynamic design practice to prevent shock waves in the compressor. This gives the need for many compression stages. (Ramgen Power Systems, 2014)

Pressure increases in multi staged centrifugal compressors diffusers, as shown in figure 5 (Air Compressor Works, Inc., 2015). Spinning impellers accelerate the fluid flow velocity and diffusers have smaller flow area, which causes flow to slow. This increasing and slowing of flow velocity causes the pressure to increase. In figure 5 is also shown main parts of a multi stage centrifugal compressor.

Aerodynamic design practice for compression is that inlet flow should be

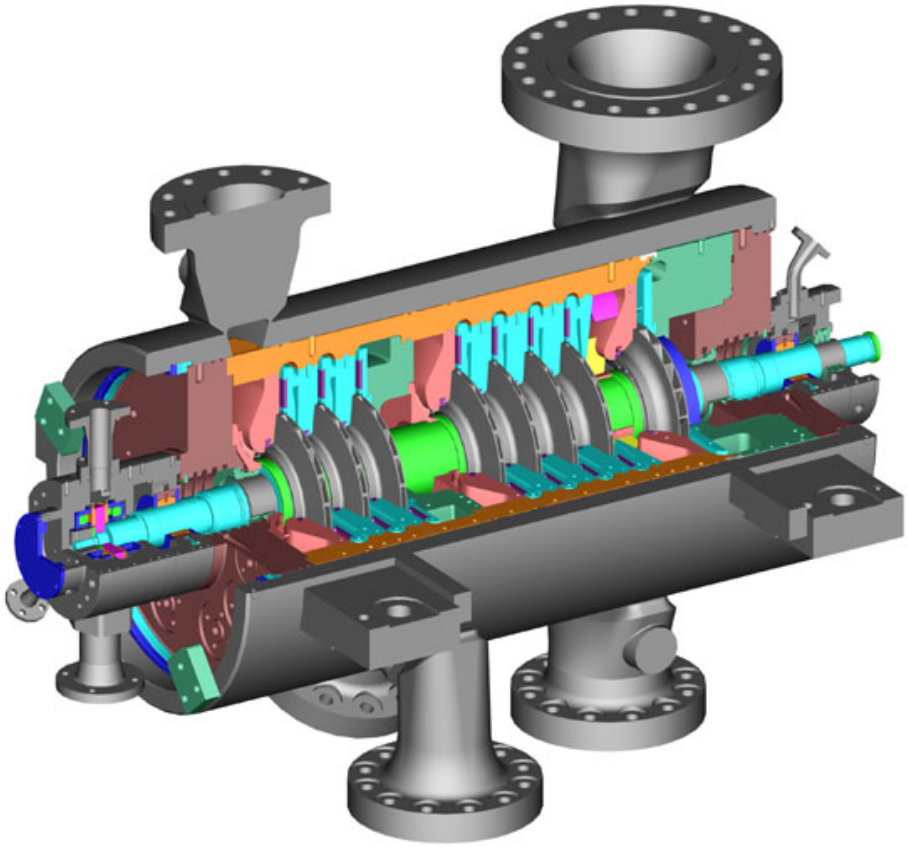

Figure 4: Multi stage single casing centrifugal compressor. (Asia Vacuum Pumps, 2015)

less than Mach 0.90. With higher Mach numbers it is possible that shock wave in the blade passages will choke the compressor causing steep drop in head and efficiency of the compressor. The Mach number is a ratio of speed of an object moving through a fluid and the local speed of sound. Local speed of sound is a function of molecular weight

$$c = \sqrt{\frac{k\mathrm{R}_u T}{\mathrm{M}}} \tag{1}$$

Where:

c	speed of sound
k	ratio of specific heats c_p/c_v
R_u	universal gas constant
T	gas temperature
M	molecular weight of the gas

Carbon dioxide has larger molecular weight than air, thus by equation (1) speed of sound in CO_2 is smaller than in air. For this reason Mach 0.9

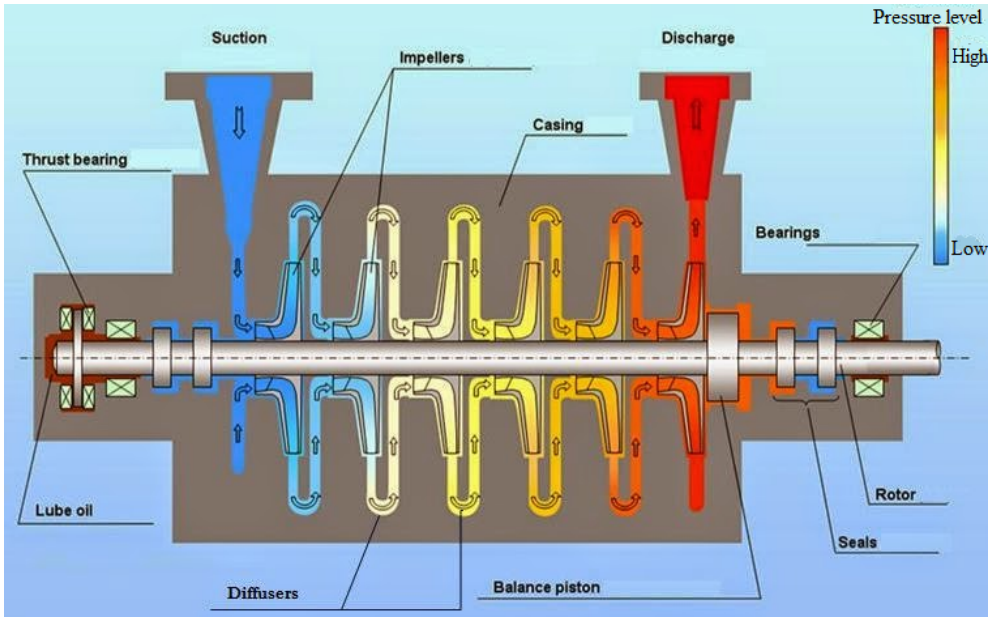

Figure 5: Simplified picture of flow path and pressure increase in a multi stage centrifugal compressor. (Air Compressor Works, Inc., 2015)

is achieved with smaller inlet flow velocities in CO_2 than in air. This limits the pressure ratio for CO_2 centrifugal compressors from 1.8 to 2.8. Typically with these stage pressure ratios eight stages of compression are needed to achieve an overall pressure ratio of 100:1. Adiabatic efficiency for these compressors range from 82 to 85%. With higher grade stainless steel it is possible to get pressure ratio close to 4.0 per stage with efficiencies of 82 to 83%, with titanium pressure ratio of 4.5 is achievable with efficiencies of 75 to 80%. (Ramgen Power Systems, 2014)

Pressure ratio is a function of the impeller exit tip speed. Impeller stresses limit the impeller tip speed at the exit of the impeller. Thus with higher grade materials it is possible to get higher pressure ratios. (Hill and Peterson, 1965) Also a higher Mach number leads to narrower operation area for the compressor, surge and choke points locate closer to the design point. Peak efficiency is smaller and the efficiency peak is pronounced. (Lüdtke, 2004) In figure 6 is shown a simplified compressor map where can be seen efficiency areas and surge and choke lines (modified from (Celica Tech, 2015)). Curves with points are different rotational speeds. Design point for compressor is usually in the middle of the highest efficiency area.

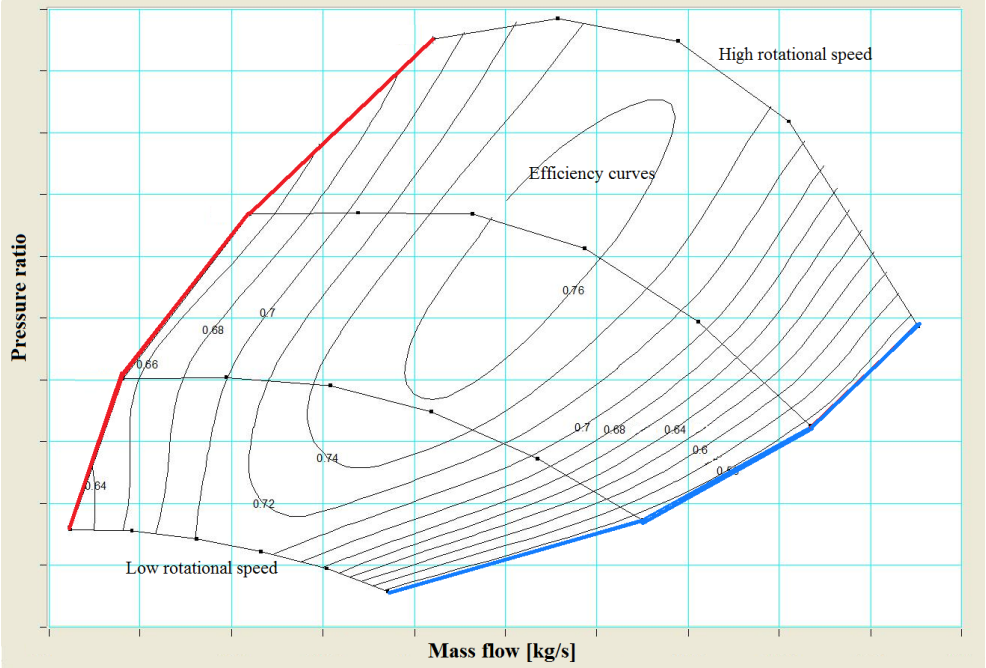

Figure 6: Simplified compressor map where can be seen how efficiency is proportional to mass flow and to pressure ratio. Red line is surge line and blue line is choke line. Modified from figure by Celica Tech (2015)

2.3 Compression

In this section are presented paths how to get to wanted pressure and temperature levels of liquid or super critical CO_2. Mainly there are two ways to reach to the desired conditions. Compression in multiple stages with inter cooling between them, or compression to high enough pressure that cooling will condensate CO_2 to liquid and then pumping it to desired pressure. To keep it more simple the captured gas stream is thought to consist only CO_2. Because of this there are not presented any impurity removal equipments. Also captured CO_2 rich stream is thought to come to the first compression stage at atmospheric pressure and temperature.

Straight compression can be done in two ways. High compression ratio path, where there is only few compression stages with inter cooling between them (see figure 8 by Moore et al. (2007)). Problem with this path is that it has low thermal efficiency and high power consumption. Figure 7 by Moore et al. (2007) shows that by increasing the number of compression stages with after-coolers, semi-isothermal compression path is possible. This is done to minimize heat of compression and power consumption. Usage of integral gear centrifugal compressors, that allow up to eight compression stages with constant pressure ratio between them in

single casing, minimizes capital costs. The semi-isothermal compression with integral gear compression is superior compared to high compression ratio approach in terms of capital costs and energy efficiency. The semi-isothermal compression approach is feasible for all large-scale CO_2 sources. (Maramba and Bhattacharya, 2011)

Compression pumping path can also be divided in to two, compression and supercritical pumping and compression with liquid pumping. In compression with supercritical pumping CO_2 is compressed above critical pressure (73.9 bar) of CO_2, CO_2 becomes dense-phase fluid. Dense-phase fluid is then pumped to desired pressure. This approach is useful when desired pressure is over 200 bar and there is no full-scale refrigeration unit available. For industrial CO_2 sources, supercritical pumping path is feasible. When there is full-scale refrigeration system available, for example cryogenic system at LNG plant, it is feasible to pump CO_2 to desired pressure in liquid phase (figure 8). First CO_2 is compressed over triple-point pressure (5.2 bar), to prevent dry ice formation, then condensed with optimal refrigerant. Condensed CO_2 is then pumped to pressure desired. (Maramba and Bhattacharya, 2011)

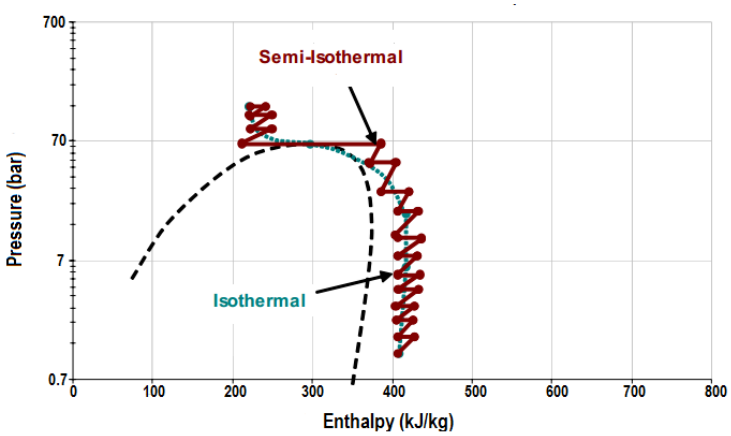

Figure 7: Isothermal (ideal) and semi-isothermal compression of CO_2 from 1 bar to 150 bars on pressure enthalpy diagrams. (Moore et al., 2007)

Inter-cooling between compression stages is done to reduce the energy consumption of compression and to condense water. Compression energy consumption increases with hotter fluid because of increase in suction volume. Cool fluid for inter-cooling heat exchanger can be water or some common refrigerant such as NH_3, CO_2, C_3H_8 and R134a. (Alabdulkarem et al., 2012) In their study Duan et al. (2013) used ammonia as a refrigerant for CO_2 stream. Ammonia vapor is boiled of from am-

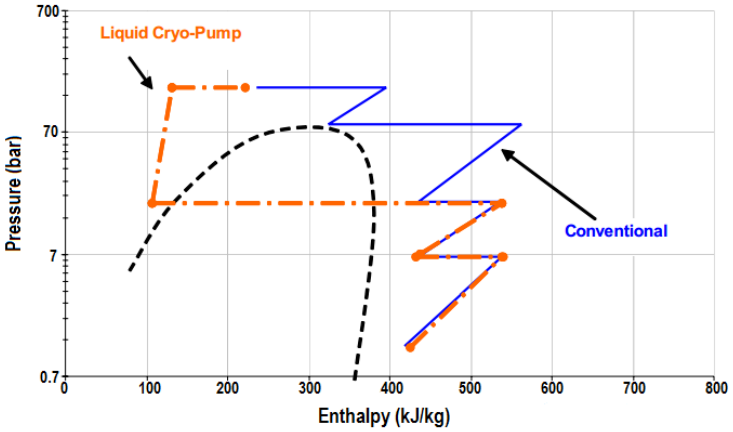

Figure 8: High pressure ratio compression (conventional) and compression liquid pumping paths of CO_2 from 1 bar to 150 bars on pressure enthalpy diagram. (Moore et al., 2007)

monia rich solution with waste heat. Ammonia vapor is then purified and cooled to liquid with water cooler. Liquid ammonia is overcooled with low-temperature ammonia coming from heat exchangers. Ammonia is cooled to -40 °C temperature in expansion valves before CO_2 heat exchangers. Colder cooling agent makes it possible to turn CO_2 in to liquid at lower pressures. With -40 °C coolant CO_2 turns liquid at about 10 bar pressure. Less compression work and more pumping means energy saving. When CO_2 is pumped to pressure desired, but temperature is lower than transportation temperature, the cold energy in CO_2 can be saved by cooling incoming CO_2 gas stream. (Duan et al., 2013) The flowchart of Duan et al. (2013) process is in figure 9.

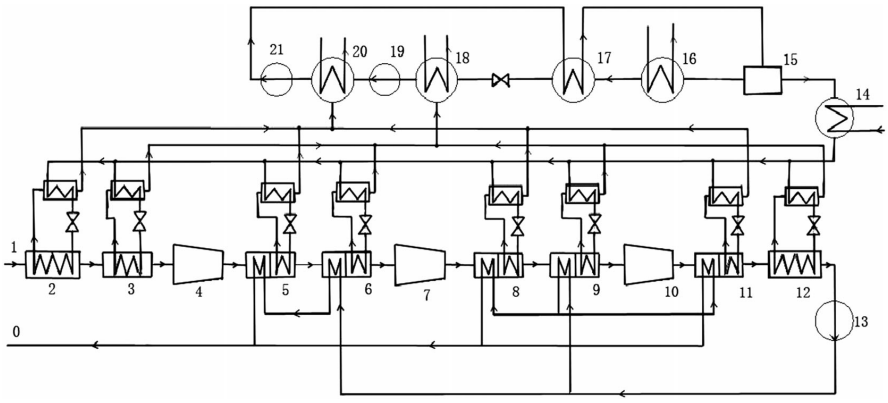

Figure 9: The flowchart of CO_2 compression with ammonia refrigeration and cool energy recovery. Explanations: heat exchangers (2, 3, 5, 6, 8, 9, 11, and 12), compressors (4, 7 and 10), ammonia (21 and 19) and liquid CO_2 (13) pumps, absorbers (18 and 20), solution heat exchanger (17), solvent generator (16), rectifying column (15) and ammonia cooler (14). (Duan et al., 2013)

When there is waste heat available CO_2 liquefaction is best to execute with ammonia absorption chiller (Alabdulkarem et al., 2012, Duan et al., 2013). When there is no waste heat available Alabdulkarem et al. (2012) suggest that CO_2 liquefaction should be integrated with refrigerant cycle at 50 bar liquefaction pressure combined with cool energy recovery from liquid CO_2. At 50 bar pure CO_2 turns liquid at 14 °C. (Alabdulkarem et al., 2012) These results can be used to reduce energy and efficiency penalties caused by liquidization, but every CCS case should be optimized specifically (Romeo et al., 2009). Comparison of different CO_2 liquidization methods is done in sections 5 and 6 with constructed dynamic models.

3 TRANSPORTATION

There are many ways to transport CO_2, motor carriers, railway, water carriers and pipelines. Results by Svensson et al. (2004) indicate that there is only three economically affordable solutions: water carriers (off shore), pipelines (on and off shore) and combination of these two. For this reason only pipeline and water carrier (ship) solutions are presented in this thesis. Main focus is on temperature, pressure and purity levels of these transportation methods, thous are in straight contact with liquidization of CO_2.

3.1 Pipeline

To economically transport carbon dioxide in a pipeline the initial pressure should be as high as possible in respect to material strength, so that number of booster stations is minimized. Pressure levels typically varies from 85 bar to 150 bar. Upper limit is due to economical material strength, lower limit is set by the phase behavior of CO_2 (see figure 2). Forbes et al. (2008) If pressure drops under critical pressure of CO_2 two phase flow occurs, this decreases the density of the fluid and causes choking to the pipe. To prevent this there are booster stations to increase the pressure of the CO_2 stream. (Zhang et al., 2006)

Temperature levels of CO_2 in pipeline varies typically from 13 °C to 44 °C. The upper limit is to prevent wearing of the external pipeline coating material. Also discharge temperature of the compression-station determines the upper temperature. (Forbes et al., 2008) Study by Zhang et al. (2006) indicate that CO_2 should be transported in sub cooled state to result significant energy savings. For sub cooled liquid CO_2 the temperature needs to be lower than 20 °C. Then pressure boosting can be done with pumps, also pipe diameter can be smaller than for supercritical transportation. This method is especially useful in cold climates where there is no need for refrigeration or insulation of the pipeline to keep the temperature as low as wanted. (Zhang et al., 2006)

For pipeline transportation volatiles, like nitrogen and argon don't account any safety or operational problems. But in sense of energy requirements it's sensible to remove these volatiles. 1 mol% of nitrogen

will increase energy requirements on transportation chain approximately 1 %. This a optimization problem, because increasing the purity level of CO_2 stream will increase the energy and capital costs of the process. (Aspelund and Jordal, 2007)

To prevent corrosion in the pipeline, the water concentration needs to be below 50 ppm. CO_2 and water can form corrosive carbonic acid in the pipeline if the water concentration is higher. Also possibility of hydrates formation is possible if the thermodynamic conditions are right, hydrates can cause plug in the pipeline. (Forbes et al., 2008)

On his masters thesis Bilsbak (2009) has combined together purity levels for different substances for pipeline transportation, based on ENCAP CO_2 (ENhanced CAPture of CO_2) project report. These purity levels are presented in table 3. For comparison on table 4 are purity levels presented by Forbes et al. (2008). These purity levels are based on North American already existing pipeline transportation levels.

Table 3: CO_2 purity levels for pipeline transportation based on report by ENCAP (2008). (Bilsbak, 2009)

Component	Design case	EOR[1]case
CO_2	>90 %	>90 %
H_2O	<500 ppm	<50 ppm
SO_2	Traces	<50 ppm
NO	Traces	Traces
H_2S	<1,5 %	<50 ppm
CO	Inerts lump	Inerts lump
Inerts lump	<4 %	<4 %
O_2	Inerts lump	100 ppm
HCN	Traces	Traces
COS	Traces	<50 ppm
Mercaptans	Traces	<50 ppm
NH_3	Traces	Traces
Hg	Traces	Traces

[1] enhanced oil recovery, see section 4.1

ENCAP design case on table 3 is for cases with CO_2 storing in geologic formations. For EOR the used CO_2 stream needs additional cleaning to meet the stricter requirements of EOR. (ENCAP, 2008) On table 4 purity levels of Type II are mostly used, Type I pipelines don't exist but can be developed for specific single use, Type III has relaxed composition standard for cases where extra operational precautions are done to

Table 4: CO_2 purity levels for pipeline transportation, already used in North American EOR projects. (Forbes et al., 2008)

Parameter	Type I	Type II	Type III
CO_2—% by volume	>95%	>95%	>96%
H_2S—ppmbw[1]	<10	<20	<10,000
Sulphur—ppmbw	<35	<30	-
Total hydrocarbons—% by volume	<5	<5	-
CH_4—% by volume	-	-	<0.7
C_2 + hydrocarbons—% by volume	-	-	<23,000
CO—% by volume	-	-	<1,000
N_2—% by volume/weight	<4	<4	<300
O_2—ppm by weight/volume	<10	<10	<50
H_2O—ppm by volume	<25	<30	<20

[1] ppm by weight

prevent leaks from the source and the sink (Forbes et al., 2008).

3.2 Ship

To transport large amounts of CO_2 efficiently with a ship, the density of the gas must be high. LNG ships transport their cargo in liquid phase at atmospheric pressure. For CO_2 this is not possible when the triple point is at 5.2 bar and −56.5 °C. Under these pressures and temperatures CO_2 exist either as vapor or in solid. In theory CO_2 can be transported in solid state with density approximately 1500 kg/m^3, but this is not feasible mainly due to difficulties of loading and unloading procedures.(Aspelund et al., 2006)

CO_2 is in liquid phase at pressures between 5.2 bar and 73 bar (from triple point to critical point). Temperature on triple point is −56 °C and on the critical point it is 31 °C. Due to this temperature difference the density of CO_2 on this interval varies from 1200 kg/m^3 at the triple point to 600 kg/m^3 at the critical point. Thus almost two times more CO_2 can be transported at pressures close to triple point than at pressures close to critical point. Low pressure is also beneficial for ship design, no need for high strength vessels. When operating close to triple point pressures can lead to operating problems. If the pressure is reduced below triple point dry ice formation can occur. When first nucleons of dry ice has formed the rest will form rapidly, in seconds. To prevent dry ice formation and to keep the density of CO_2 as high as possible, the ship transportations

are done in pressure close to 6.5 bar and temperature close to −52 °C. (Aspelund et al., 2006)

For ship transportation the CO_2 is first pressurized to 15-20 bar pressure. At these pressures water separation can be done efficiently. Water is removed to prevent hydrates, freezing of water and corrosion. Also lowest preferable pressure for CO_2 condensation is at this pressure interval. After water separation and condensation the liquid CO_2 is expanded to transportation pressure in one or two stages. (Aspelund et al., 2006) High volatile content will increase the risk for dry ice formation, because these volatiles work as nucleons where dry ice starts to form. (Aspelund and Jordal, 2007) Requirements for purity levels made by ENCAP (2008) are presented in table 5 constructed by Bilsbak (2009). These ship transportation purity levels are for case where transported CO_2 is used in EOR (ENCAP, 2008).

Table 5: CO_2 purity levels for ship transportation based on ENCAP report. (Bilsbak, 2009)

CO_2	>95 %
H_2O	<5 ppm
SO_2	<5 ppm
NO	<5 ppm
H_2S	<5 ppm
CO	<5 ppm
Inerts lump	<4 %
O_2	100 ppm
HCN	5 ppm
COS	5 ppm
Mercaptans	10 ppm
NH_3	Traces
Hg	Traces

Because with ships the transportation can't be continuous, there is a need for onshore storage. Aspelund et al. (2006) designed on their paper these ground storages to have total capacity of 1.5 times the ship capacity. Commonly these storage tanks are semi-pressurized spheres, semi-pressurized cylindrical tanks or underground storage in caverns. (Aspelund et al., 2006) In storage tanks CO_2 is kept in ship ready liquid phase. Ships cargo tanks are first filled with pressurized gaseous CO_2 to prevent humid air contamination and the formation of dry ice, before the liquid CO_2 is pumped in. When liquid CO_2 is unloaded the cargo tanks

are filled with dry gaseous CO_2 to prevent tanks contamination of humid air. (IPCC, 2005)

4 CO_2 STORING AND UTILIZATION METHODS

Carbon dioxide has many possible storing and utilization methods. Most of these methods are presented in figure 10 (NETL, 2014). This section covers only couple of storing and utilization methods from this wide range of processes. Special attention is focused on the pressure and temperature levels and on the composition of CO_2 used in the processes.

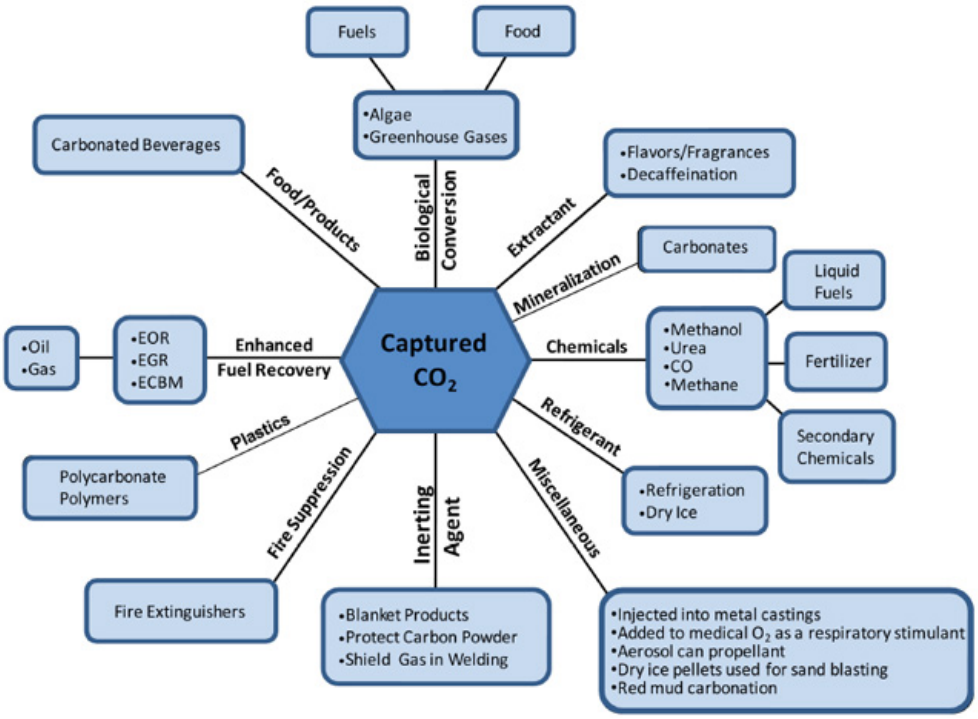

Figure 10: Schematic to show the utilization possibilities for CO_2. (NETL, 2014)

4.1 Enhanced oil recovery (EOR)

Enhanced oil recovery is a CO_2 storing and utilization method, where CO_2 injected into the oil well will increase the oil production. Every ton of carbon as CO_2 injected into the oil well will produce approximately 2.8 tons of carbon as oil. (Holloway, 2001) Injected CO_2 increases the pressure in the oil reservoir extracting residual oil while the injected CO_2 stays stored in the reservoir (Leung et al., 2014).

The fact that oil reservoirs have already held hydrocarbons for millions

of years, gives confidence that they can store CO_2 for times to come. First EOR projects were implemented in 1972 and in 2000 already 84 commercial EOR projects were operational worldwide. USA is the technology leader and has 72 from these 84 projects, yearly these 72 projects inject over 30 million metric tons of CO_2. (Herzog, 2011) After the EOR project has ended the injection of CO_2 can be continued to maximize CO_2 storage in the depleted field (Hill et al., 2013).

Purity standards for injected CO_2 are shown in tables 3 and 5. In EOR operations impurities in CO_2 stream may affect the oil recovery, because they change the solubility of CO_2 in oil, this decreases the ability of CO_2 to vaporize oil components. CH_4 and N_2 decreases the oil recovery rate, where H_2S and heavier than methane hydrocarbons have the opposite effect. SOx also may improve oil recovery when NOx can decrease miscibility and thus reduce the oil recovery. Oxygen in CO_2 can react with oil exothermically causing the temperature at the injection point to rise. More studies need to be made concerning contaminants in CO_2, because there might be cost savings when CO_2 is stored with impurities. (IPCC, 2005)

Injection of CO_2 happens at pressure equal or higher than the minimum miscibility pressure (MMP). At MMP pressure CO_2 and oil mix and form easily flowing product liquid. (Ravagnani et al., 2009) MMP pressure is around 100 to 150 bar, depending on oil and CO_2 composition and reservoir temperature (IPCC, 2005). In the oil field of Permian Basin of West Texas CO_2 is boost compressed to pressure between 150 and 165 bar before injection (Meyer, 2007). If ship transported CO_2 is used for EOR, it needs to be heated before boost compression. At -50 °C temperatures many materials become brittle, flexible riser from ship to pumping platform is a problem. Cold CO_2 is heated to 10-20 °C with waste heat (if available) or with sea water (warm waters) before pumping to 200–300 bar. (Aspelund et al., 2006) Presented pressure levels used for EOR vary from 100 to 300 bar, as mentioned pressure level depends on conditions of oil well and CO_2 used.

4.2 Chemicals

110 Mt CO_2 per year is used in chemical industry, either converted into chemicals or used as a substitutive to CO in the methanol synthesis (6 Mt

CO_2 per year). CO_2 can be converted for example into urea (70 Mt CO_2 per year), inorganic carbonates and pigments (about 30 Mt per year). Super critical CO_2 is applicable as a solvent for reactions, nanoparticle or -composite production, and polymer-modification. In these technological applications CO_2 is not converted into other chemicals and can be recovered and reused. (Aresta and Dibenedetto, 2007)

As CO_2 is the end product of any combustion process where carbon is involved, it is clear that CO_2 lays in a potential energy well. This means that CO_2 is relatively inert and doesn't react too easily. To make CO_2 react it needs help from catalysis and coordination. By using electrochemical or photo assisted reduction and metal enzyme catalysis or their combination the reaction rate of the CO_2 can be increased . (Yin, 1995)

Producing methanol from CO_2 and H_2 is possible and first pilot plant in Japan produces methanol 50 kg per day. This plant uses SiO_2 modified Cu-ZnO as a catalyst. Pressure and temperature levels in this pilot plant are 50 bar and 250 °C. (Aresta and Dibenedetto, 2007) Purity levels for CO_2 used are not mentioned.

4.3 Methanation

Methanation of CO_2 has a special attention because of increasing interest of methane as a energy storage for renewable energy. Solar and wind energy processes are not constant producers and thus time to times there is over capacity of energy. This energy should be stored and used when needed. Renewable peak energies are used in electrolysis process to make hydrogen. In methanation process hydrogen from electrolysis and captured CO_2 are reacted to form methane. The main advantage of methane compared to hydrogen as a energy storage is the use of an already existing natural gas infrastructure (gas grid, etc.). Pure hydrogen can be fed only to certain concentration into the gas grid in order to keep the gas quality within specifications. Also methane is more energy dense and transport in pipeline requires less energy. The main disadvantage of methanation is the lower overall efficiency than with hydrogen. (IEC, 2011)

As mentioned in section 4.2 CO_2 is relatively inert and needs catalyst to react. Nickel-based catalysis are most widely used for methanation

reaction due to their high catalytic activity, high selectivity for methane and relatively low price (Hwang et al., 2011). Methanation reaction $CO_2 + 4\,H_2 \longrightarrow CH_4 + 2\,H_2O\ \Delta H_{298K} = -252.9\,\mathrm{kJ/mol}$ is exothermic. During the exothermic methanation process nickel-based catalysis suffer from sintering. Sintered particles have reduced catalytic activity. (Wei and Jinlong, 2011) Many studies are made to increase the stability and activity of nickel-based catalysts for methanation reaction (Hwang et al., 2011).

In their thermodynamical analysis for CO_2 methanation reaction Gao et al. (2012) have studied the effects of temperature, pressure and initial reactant compositions on the conversion of CO_2 and CH_4 selectivity and yield. CO_2 conversion is defined by equation (2), and CH_4 selectivity and yield by equations (3) and (4) respectively. Thermodynamic equilibrium analysis of the methanation reaction of CO_2 with experimental results from literature by Gao et al. (2012) indicate that high CH_4 yield is achieved at low temperature, high pressure and high H_2/CO_2 ratio. (Gao et al., 2012) These result can be seen from the figures 11 and 12.

$$X_{CO_2}(\%) = \frac{F_{CO_2,in} - F_{CO_2,out}}{F_{CO_2,in}} 100 \tag{2}$$

Where:

X_{CO_2}	CO_2 conversion
$F_{CO_2,in}$	molar flow rate of CO_2 at inlet
$F_{CO_2,out}$	molar flow rate of CO_2 at outlet

CO_2 conversion defines how many percents of CO_2 reacts in the methanation process. This is calculated by equation (2). High value means good reactivity of CO_2.

$$S_{CH_4}^{CO_2}(\%) = \frac{F_{CH_4,out}}{F_{CH_4,out} + F_{CO,out} + F_{C,out}} 100 \tag{3}$$

Where:

$S_{CH_4}^{CO_2}$	CH_4 selectivity (CO_2 methanation system)
$F_{CH_4,out}$	molar flow rate of CH_4 at outlet
$F_{CO,out}$	molar flow rate of CO at outlet
$F_{C,out}$	molar flow rate of C at outlet

CH_4 selectivity tells how well methanation process produces CH_4. High value means that mainly CH_4 is produced. Unwanted CO and C are not

produced from CO_2.

$$Y_{CH_4}(\%) = \frac{F_{CH_4,out}}{\sum_i N_i F_{i,in}} 100 \tag{4}$$

Where:

Y_{CH_4}	CH_4 yield
N_i	the number of carbon atom of species i
$F_{i,in}$	molar flow rate for products i at inlet

High CH_4 yield indicates that methanation process produces mainly CH_4 from all the carbon that is put into the process. In equation (4) i indicates all species that contain carbon at methanation process inlet. These species are CO,CO_2,CH_4 and C_2H.

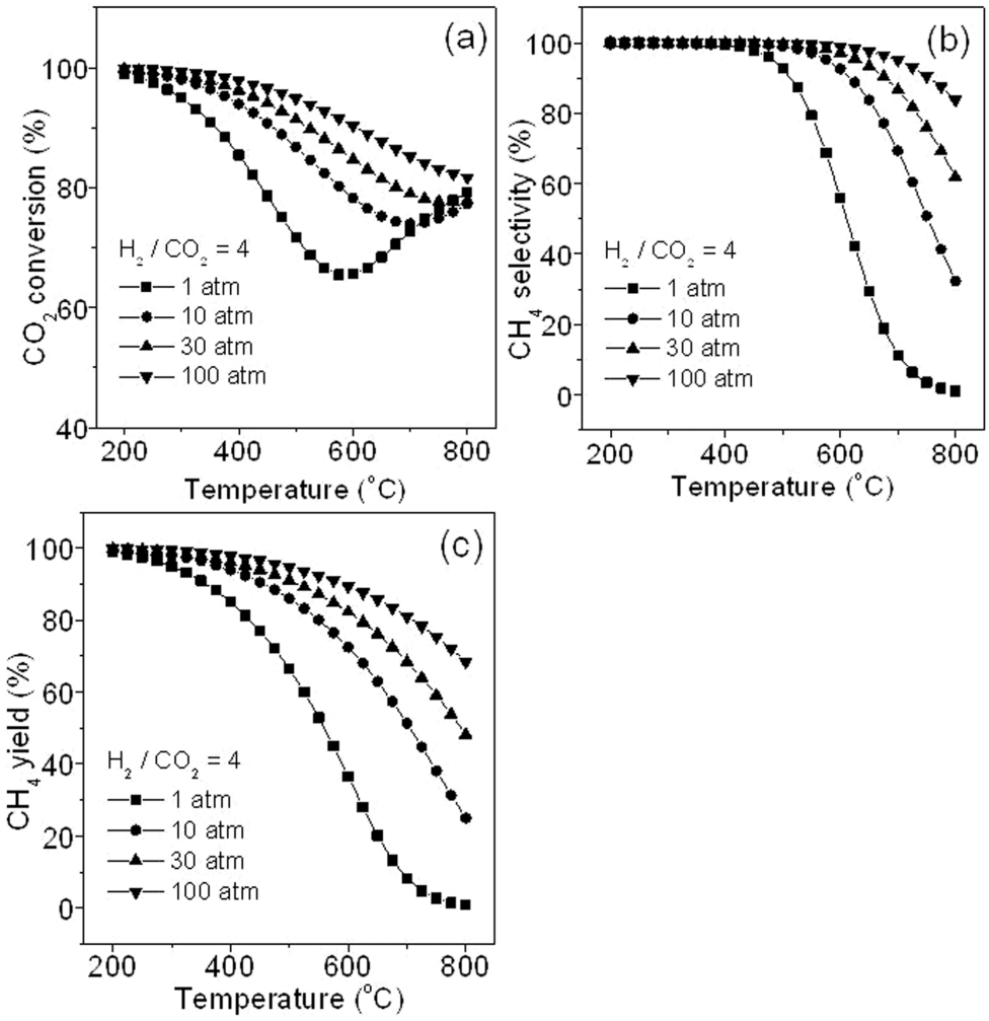

Figure 11: Effects of pressure and temperature on CO_2 methanation: (a) CO_2 conversion, (b) CH_4 selectivity, and (c) CH_4 yield. (Gao et al., 2012)

Increasing CO_2 conversion in figure 11 (a) above 600 °C is result from

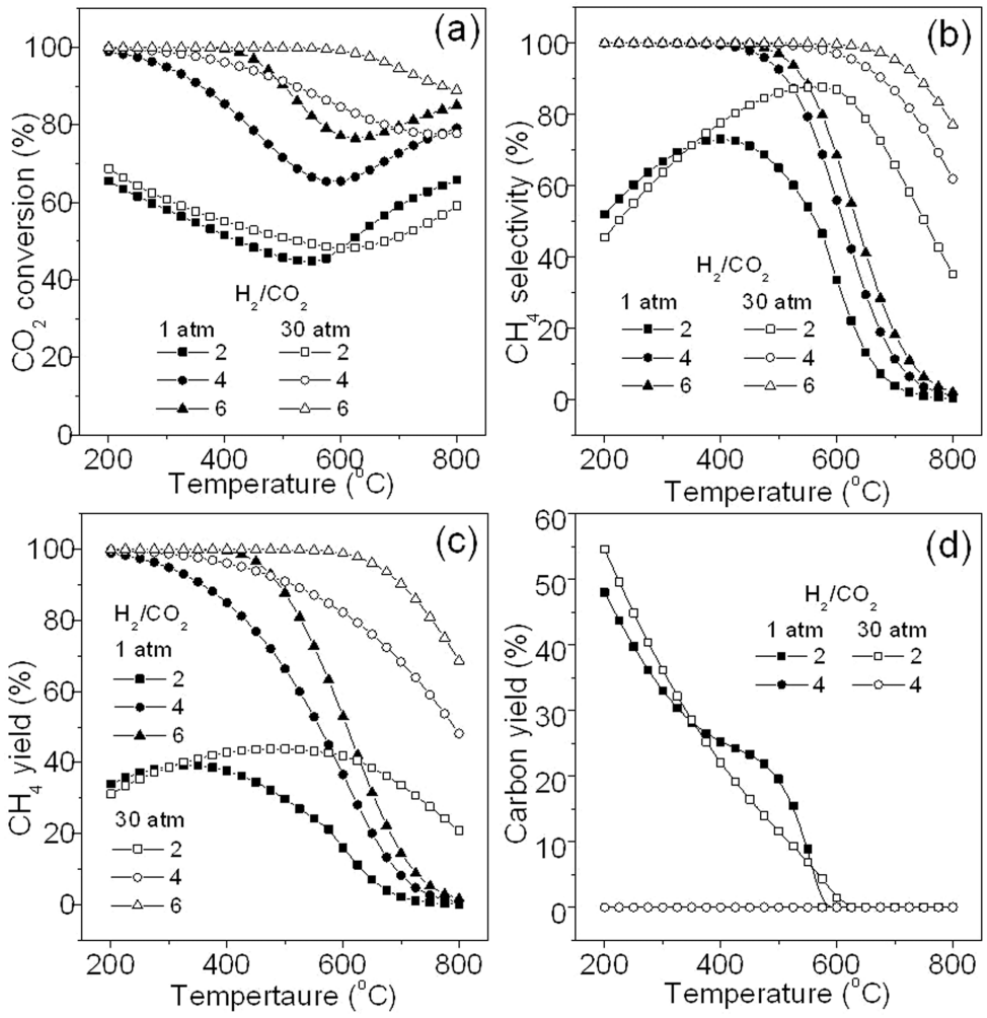

Figure 12: Effect of different H2/CO2 ratios on CO_2 methanation: (a) CO_2 conversion, (b) CH_4 selectivity, (c) CH_4 yield, and (d) carbon yield. (Gao et al., 2012)

reversed reaction $CO + H_2O \longleftrightarrow CO_2 + H_2$ (water-gas sift), which dominates at temperatures above 600 °C and consumes CO_2. To achieve high CH_4 yield and CO_2 conversion H_2/CO_2 ratio should be at least 4 (see figure 12 (a) and (c)). Also to prevent deactivation of catalysts resulting from carbon deposition on catalyst surface, the H_2/CO_2 ratio should not be lower than 4 (see figure 12 (d)). Conclusively CO_2 methanation is optimized with low temperature, high pressure and proper H_2/CO_2 ratio. (Gao et al., 2012)

H_2O in the process causes a little decrease in CO_2 conversion and no significant difference in CH_4 selectivity and yield. But steam in the feed gas could decrease the carbon deposition to a large extent. In their study Gao et al. (2012) had $H_2/CO_2/H_2O = 3/1/0.5$ ratio with no significant changes in methanation. Impurities such as O_2 and C_2H_4 should be

kept out from the process to maximize methane yield and to minimize carbon formation. Even though O_2 can lead to a reduction of carbon formation, because carbon and oxygen reacts to form CO_2. (Gao et al., 2012) Impurities in CO_2 stream may poison methanation catalyst. One of the most common poison for catalyst is sulphur, especially coming from H_2S. Sulphur is particularly severe for nickel catalysts. (Peebles et al., 1983)

4.4 Temporary storage

Temporary storage tanks are used when CO_2 can't be used right away after capture. Like mentioned already in section 3.2 concerning ship transportation, that when ship is on transportation trip the CO_2 is stored to temporary tanks. In their article Aspelund et al. (2006) have planned steel storage tank farm that consists 10 tanks. The total storage capacity is $30\,000\,m^3$. They say that the volume of the tank farm is at the upper end of the existing storage facilities. However they mention that there exists tank farms with capacities in excess of $50\,000\,m^3$, tank farms of this size have 30 or more pressure tanks. (Aspelund et al., 2006) For liquid natural gas (LNG) exists carriers reaching more than $200\,000\,m^3$ capacity (IPCC, 2005). If this size vessels are possible (pressurization needed) for CO_2 transportation the onshore storage capacity needs to be $300\,000\,m^3$.

Pressure in intermediate storage for ship transportation is kept within 6.5-7.5 bar. Lower limit has pressure margin to triple point (-56.5°C, 5.2 bar) to prevent unintended events (gas or solid formation). High pressures increase the construction cost of a tank, thus the pressure is limited from the upper end. Temperature is corresponding to pressure level that CO_2 stays in liquid phase. (Aspelund et al., 2006, Lee et al., 2012) From CO_2 phase diagram (see figure 2) it is possible to determine that on pressure interval from 6.5 bar to 7.5 bar the temperature needs to stay above -55°C to prevent solid formation but under -51.5°C at 6.5 bar and under -47.7°C at 7.5 bar to prevent vaporization.

Conditions in the storage tanks are close to boiling point, thus some vaporization happens in the tanks. Also filling and emptying the tanks influence on the tanks vapor level, pumping causes thermal heat in the liquid CO_2 causing it to boil. Filling the tanks result in a level built up

in the storage tank, this compresses the vapor phase above the liquid. If vapor is not removed the tanks pressure is building up excessively. During the filling continuous vapor stream is removed from the tank and is returned to CO_2 liquefier. Emptying the storage tanks causes pressure reduction in the tanks. Decrease of the pressure causes also decrease on temperature because of Joule-Thompson process, this may cause solidification of the tank content. On ship loading situation this can be prevented by returning the vapor from the ship to the temporary storage tank. This will prevent pressure decrease in the storage tank and pressure built up in the ship. (Vermeulen, 2011)

Heat input from the environment causes vaporization in the temporary storage tanks, resulting in pressure increase. The effect of the heat input depends on the insulation type, insulation thickness, meteorological conditions and filling level of the tank. Insulation type, insulation thickness and meteorological conditions are obvious aspects on the heat input level, thick insulation with low thermal conductivity in cold meteorological conditions slows pressure build up in the tank. Low filling level gives more space for the vapor in the tank. Vapor has lower specific heat capacity than liquid and thus it tends to heat up faster than liquid causing faster pressure build up in the tank. Temperature equilibrium between the two phases is kept by spraying liquid in the vapor space, thereby maintaining the lowest possible tank pressure. (Vermeulen, 2011)

As installation costs for temporary tanks can be significant part of the total costs in CO_2 utilization process, it is important to determinate the best operating and design conditions for the tanks. These parameters are optimized for every situation specifically. Pressure and temperature levels presented in this section are for ship transportation terminal storage tanks. For other processes these levels can be different.

5 APROS MODELS

Apros 6 Combustion software was used in this thesis for the dynamic CO_2 liquidization models. In total three models were made, straight compression model, compression with liquid pumping and compression liquid pumping model with cold recovery from liquid CO_2. Straight compression model is similar to one presented in figure 8 as conventional compression, but has more compression stages. An example of compression with liquid pumping models is also presented in figure 8. Refrigerant used in liquid pumping models was ammonia NH_3.

For all these models the boundary conditions was the same, compressing CO_2 stream from 1.1 bar to 140 bars. Inlet temperature for CO_2 was 40 °C and target for the outlet temperature was also 40 °C, but of course in model without cold recovery the outlet temperature was significantly lower. Between compressor stages the stream was cooled with water to temperature five degree higher than water temperature. Also refrigerant in refrigerant cycle was cooled with water between compressor stages.

In these models CO_2 stream was 100 % pure. Thus water removal systems between compressor stages were not modeled. Also refrigerant NH_3 used in the models was 100 % pure.

5.1 Apros modeling software

Apros is a dynamic simulation and modeling software for all kinds of processes and power plants. Apros was developed by VTT Technical Research Center of Finland and Imatran Voima Oy in 1986. Currently Apros is co-developed by VTT and Fortum Nuclear Services Ltd. Simulations for dynamical thermal hydraulic processes in nuclear and conventional power plants are possible with the program. (Hänninen and Ylijoki, 2008)

Apros allows modeler to combine process modeling with automation modeling. This makes it possible to see how the process and the automation works together. The whole integrated system is then possible to study and optimize in detail. (Apros web page, 2014)

On Apros 6 the user has access to a set of predefined process component

models that are conceptually one-to-one analogous with concrete devices (compressors, pumps, valves etc.). These process components hide all solution algorithms. The user only selects appropriate process components from the model library, connects them together and enter proper input data for the process. The Apros simulation models are structured hierarchically as presented in figure 13. (Apros User Manual, 2014)

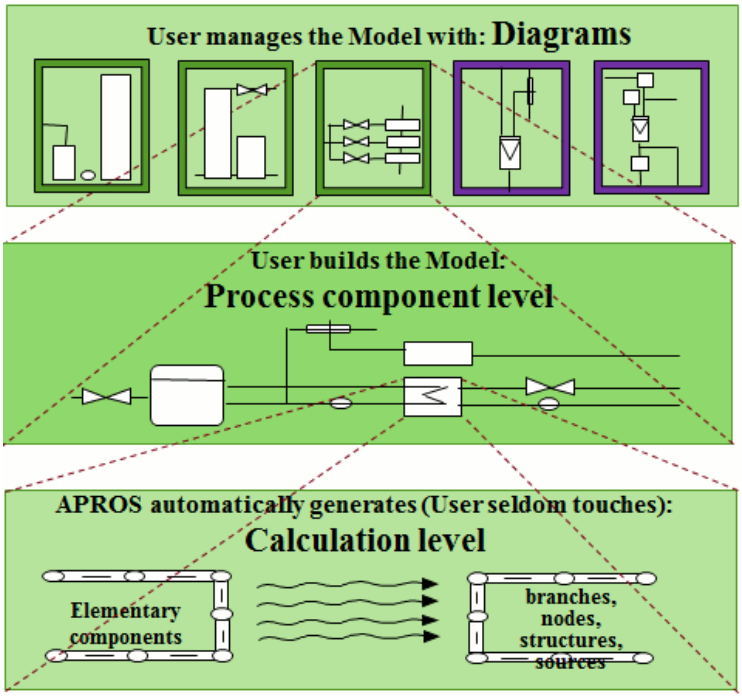

Figure 13: Hierarchical structure of a Apros model. (Apros User Manual, 2014)

The number of diagrams in one Apros process model is not limited. Usually automation modeling is set to its own diagram(s) and the actual process is in another diagram(s). Normally the user operates on the process components level using predefined process components to construct the simulation model. On Apros 6 the simulation model is configured graphically through a CAD-like Apros Modeller user interface. Process components automatically generate the calculation level objects called nodes and branches. (Apros User Manual, 2014)

The thermohydraulics package of Apros model is based on dynamic conservation equations of mass, energy, momentum and component mass fractions. Means for solving furnish mixture flows, heat conduction in solid structures and heat conduction between fluids and structures are provided by the thermohydraulics package. When solving the conservation equations the model is considered as a network of nodes (control

volumes) and branches (connections between nodes). Process component models automatically manage this network. This generates the calculation level components, which attributes are deduced from the properties of the process components. For example branch loss coefficients are solved by valve models. For thermohydraulic nodes the primary state variables are pressure, enthalpy, and component mass fractions, and for branches flow velocity. According to pressure, enthalpy and component mass fractions various quantities such as density and viscosity are calculated by material property functions. (Apros User Manual, 2014)

Differential conservation equations are discretized with respect to space and time and the non-linear terms are linearized. Staggered discretization scheme is used in the space discretization. The mass and energy equations are solved in the same nodes, while the momentum equation is located in branches. The state variables (pressure, enthalpy etc.) are calculated in the middle of the mass and energy mesh cells and the flow related variables (velocities for instance) are calculated in the momentum mesh cells. The first order upwind discretization scheme is used for the enthalpy solution. (Hänninen and Ylijoki, 2008)

5.2 Model automation

For all the models automations were done with simple PI controllers (proportional-integral controllers) combined with different kinds of measurements and actuators. CO_2 mass flow was set to value desired by controlling compressors rotational speed. Mass flow after every compressor stage was monitored and every compressors rotation speed was controlled so that mass flow stays at the set point value. Temperatures before compressors were measured and cooling water mass flow was adjusted with control valve controlled by pneumatic valve actuator to keep the temperature at desired value. Pressure after cooling water pump was kept on 3 bars to make sure that there is always enough pressure that cooling water keeps running to the right direction. Apros model automation components that were used in the models are shown in figure 14.

Power consumption of every compressor stages was monitored with analog calculations to make sure that build-in calculations in Apros work properly as the CO_2 gets close to the critical point. For the analog calculations the variables needed in the compressor power equation (5) were

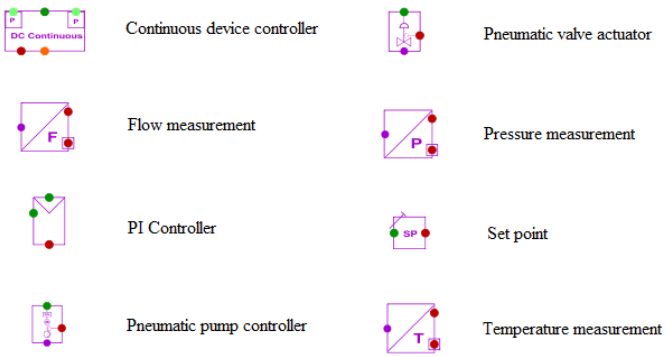

Figure 14: Apros model automation components used in the models.

measured for every compressor stage separately. Concern with build-in calculation was that at the critical point CO_2 specific heat goes to infinity and this could cause unrealistic values for compressor power. During the simulations there wasn't significant difference between the build-in calculations and analog calculations. Calculations in Apros can handle discontinuous values at the critical point.

$$P_{comp} = q_m c_p T_1 \left(\frac{p_2}{p_1}^{\frac{R}{c_p \eta_p}} - 1 \right) \tag{5}$$

Where:

q_m	mass flow
c_p	mean isobaric specific heat over compressor
R	specific gas constant
T_1	inlet temperature
p_1	inlet pressure
p_2	outlet pressure
η_p	polytropic efficiency of the compressor

Equation (5) is for ideal gas. This can cause significant error in results and it should be noticed. In general deviation between real gas and ideal gas becomes more significant closer the gas is a phase change, lower the temperature or the larger the pressure. Now CO_2 is compressed to high pressure and it experiences a phase change. To account real gas behavior to ideal gas law compressibility factor Z should be used. Compressibility factor is defined by equation (6).

$$Z = \frac{V_m}{V_{m,ideal}} = \frac{pV_m}{RT} \tag{6}$$

Where: V_m molar volume

$V_{m,ideal}$ molar volume of the corresponding ideal gas

For CO_2 compressibility factor in respect to pressure and temperature can be seen in figure 15. Close to the critical point compressibility factor goes close to 0.2. This means for example that density calculated with ideal gas law is only 20% of the value corrected with compressibility factor.

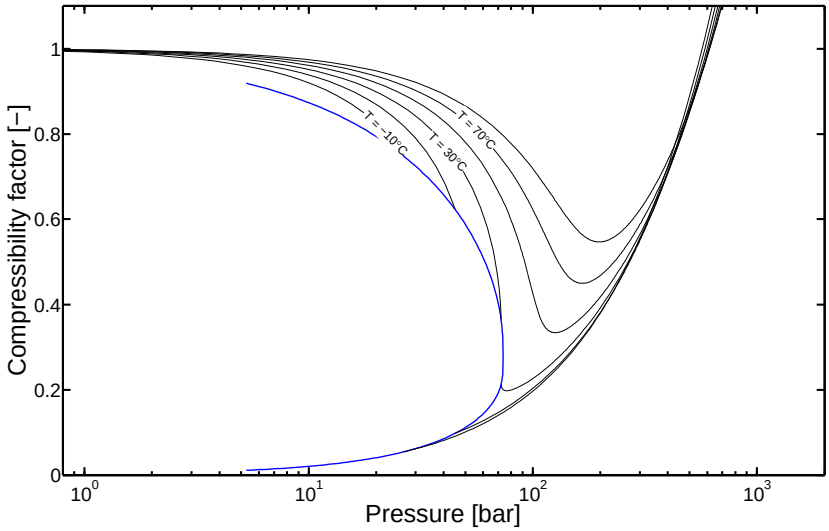

Figure 15: Compressibility factor for CO_2 in respect to pressure and temperature, saturation line with blue.

In Apros calculations are based on tabled real values of pure fluids. For this reason mixtures couldn't be used in the models. But this also means that Apros is not using ideal gas assumption in its calculations, for example densities are taken from tables instead of calculated. Of course interpolating values from table causes small error, but it should be negligible.

5.3 Model designs

Models are build with Apros process components presented in figure 16. Main components in the models are compressors, control valves, pumps and heat exchangers. Check valves are used for just in case purposes to prevent inverse flows at low mass flow situations when compressors might surge and be inefficient. Points are needed in the calculation level of the Apros and to form the connections between components. Pipes are

giving dimensions for the models. Mass flow measurements are mainly taken from the pipes.

Nominal CO_2 mass flow for all the models was 12 kg/s. Nominal cooling water temperature was 35 °C, thus the nominal inlet temperature for the compressors was 40 °C. Cooling water temperature was thought to be so high to ease the result comparison with Alabdulkarem et al. (2012). Nominal state parameters used for the CO_2 compressors in the models are collected together in table 6. In addition to these the inlet pressures and flow areas for every compressor stages were also set. Inlet pressures were set after short simulation run to thous calculated by Apros at the connection points before compressor stages. Flow areas were set so that flow velocity in the compressor stage has sensible value. As the CO_2 gets more dense the compressors flow area gets smaller. Also surge margin was monitored for the compressor stages when flow areas were chosen. Surge margin is a measure of how close an operating point is to surge and it is usually given in percentage by equation (7). Designed surge margin for every compressor stage was 30%, some differences to this was allowed as getting exact value was difficult.

$$SM = 100\% \left(\frac{q_{m,w} - q_{m,s}}{q_{m,s}} \right) \tag{7}$$

Where:

$q_{m,w}$ operating point mass flow

$q_{m,s}$ surge point mass flow

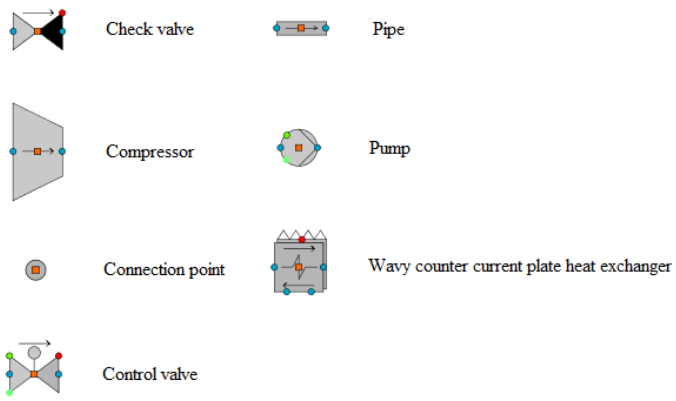

Figure 16: Apros model process components used in the models.

Predefined Apros compressor characteristics were used for all compressor stages in CO_2 and NH_3 compressors. Simplified compressor charac-

Table 6: Nominal state parameters for CO_2 compressors.

	Unit	Nominal value
Inlet temperature	°C	40
Mass flow	kg/s	12
Polytropic efficiency	%	80
Rotational speed	1/s	50

teristic taken from Apros manual is shown in figure 17. Apros creates compressor characteristics from two point pairs which are connect by second order curve, that has vertex in the first point and goes through the second point. These point pairs are generated around compressors nominal state mass flow and pressure ratio in a way that second point in second to last curve in figure 17 is the nominal state point. Apros generates point pairs so that first point is at zero mass flow for every rotation speed. This means that in Apros compressors aren't surging even with unrealistically small mass flow rates. User given characteristic could be given to Apros, but it wasn't done because from literature was not found any CO_2 compressor characteristic. Also compressor characteristic in Apros don't have efficiency curves in it, as was in figure 6. Thus Apros is not changing the compressor efficiency when mass flow is changed. This causes unrealistic results when part loads are modeled with Apros.

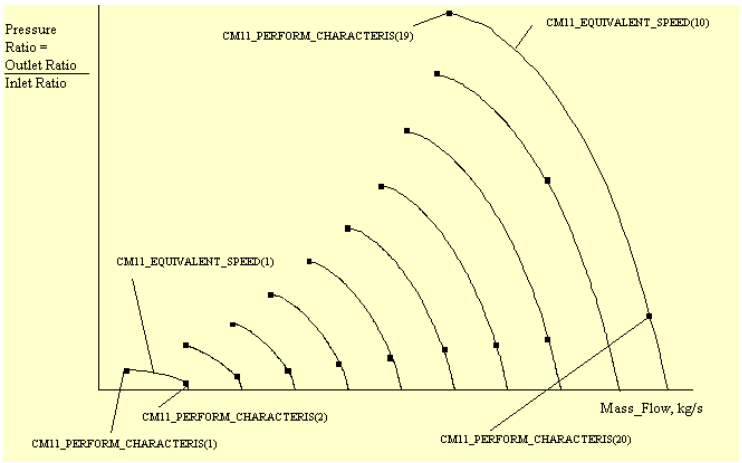

Figure 17: Simplified compressor characteristic, Apros generates compressor characteristics based on point pairs (black dots). Point pairs are scaled from nominal mass flow and pressure ratio. (Apros User Manual, 2014)

Flow areas in all of the valves, pipes and pumps were set so that the flow velocity at the nominal state has value from 1 to 3 m/s for liquids and 10 to 13 m/s for gases. Control valves in cooling water line were dimensioned

to have the valve set point at around 0.5, to make it possible to get more or less cooling water in to the heat exchangers if needed. Nominal head for the cooling water pump was 50 m even tough it was set to do only 20 m head. Liquid CO_2 pumps had nominal head of 1250 m which is the difference between 140 bars and 15.5 bars for liquid with density of 1000 kg/m^3. CO_2's density at 15.5 bar and -33 °C is about 1080 kg/m^3, thus CO_2 pumps were producing about 1170 m head. Isentropic efficiency for all the pumps used in the models was 75 % (water and liquid CO_2).

At the nominal state the heat exchangers were modeled to have 0.1 bar pressure drop. Pressure loss in heat exchanger canals is a function of flow velocity. Appropriate flow velocity and reasonable pressure drop was achieved by altering the flow areas in heat exchanger canals. Pinch temperatures for the heat exchangers were 5 °C. Heat exchangers heat transfer areas were chosen so that this pinch temperature was achieved. In table 7 is gathered main user defined parameters for process components.

Stage specified in table 7 means that value is specified specially for every stage by the methods mentioned earlier. Control valves are place specified, as they are used in CO_2 line, as NH_3 expansion valve and in cooling water line. In every case control valve has its special purpose and thus place specified values. From parameters in table 7 and boundary conditions for the process are calculated parameters, such as heat transfer coefficients for heat exchangers and flow velocities in pipes and valves etc. Mainly, if value is not shown in table 7 it is calculated, some exceptions are of course.

5.3.1 Straight compression

Straight compression model is the simplest model for the CO_2 liquidization. Model consists only compressor stages having heat exchangers between them, as presented in figure 18. On the figure 18 is the first two compressor stages of the Apros model, model continues similarly for six more compressor stages. After the last compressor stage is a heat exchanger that drops the outlet temperature to 40 °C. Analog compressor power calculations aren't shown in figure 18.

Pressure ratio for the compressor stages used in the model was 1.86. This

Table 7: Main user defined parameters for main process components used in the models. Compressor values are for CO_2 compressors.

	Unit	Value
Compressor		
Inlet temperature	°C	40
Inlet pressure	bar	stage specified
Nominal mass flow	kg/s	12
Pressure ratio	–	1.86[a]/2[b]
Rotational speed	rpm	3000
Flow area	m^2	stage specified
Polytropic efficiency	%	80
Mechanical efficiency	%	99
Heat exchanger		
Thickness of one plate	mm	1
Breadth	m	stage specified
Length	m	stage specified
Plate distance	mm	stage specified
Number of plates	–	stage specified
Nominal pressure loss	bar	0.1
Pinch temperature	°C	5
Material		stainless steel
Pump		
Flow area	m^2	0.01/0.1
Nominal volumetric flow	m^3/s	0.011
Nominal density	kg/m^3	1080[c]/1000[d]
Nominal head	m	1250[c]/50[d]
Maximum head	m	2000[c]/100[d]
Control valve		
Flow area	m^2	place specified
Nominal mass flow	kg/s	place specified
Nominal pressure loss	bar	place specified
Nominal density	kg/m^3	place specified

[a] straight compression model
[b] other models
[c] CO_2 pump
[d] cooling water pump

is calculated by dividing the total pressure ratio of 140:1.1 equally to the compressor stages. Also pressure losses in the heat exchangers are taken into account.

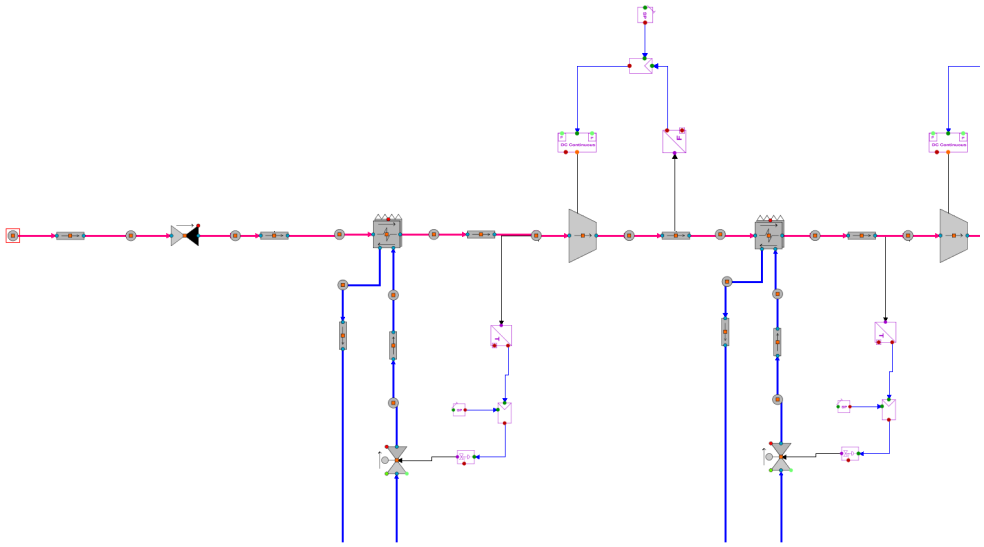

Figure 18: Simplified Apros diagram of the straight compression model's first two compressor stages. Red line is for CO_2 and blue is cooling water.

Straight compression liquidization path is presented in pressure–enthalpy diagram on figure 19. Whole compression is done at the superheated region CO_2 with big margin to the vapor dome. With cooler cooling water the process would move closer to the vapor dome, but it should be kept in mind that the CO_2 need to stay in gas phase when compressors are used.

5.3.2 Compression liquid pumping

To make it possible to liquidize CO_2 by cooling it needs to be at pressure higher than triple point pressure (5.2 bar). For the Apros model it was chosen that CO_2 is compressed to 15.5 bar pressure before it is liquidized by cooling. This pressure was controlled with CO_2 pump rotation speed. Increasing the rotation speed will decrease pressure after the compressors as the pump does more pressure and vise versa. Pressure was raised to 15.5 bars with four compressor stages each having pressure ratio of 2. Between the compressor stages the CO_2 was cooled with water like in previous model. Nominal values for the compressor stages were the same as in table 6.

Liquidization cooling for CO_2 was done with NH_3. Temperature before

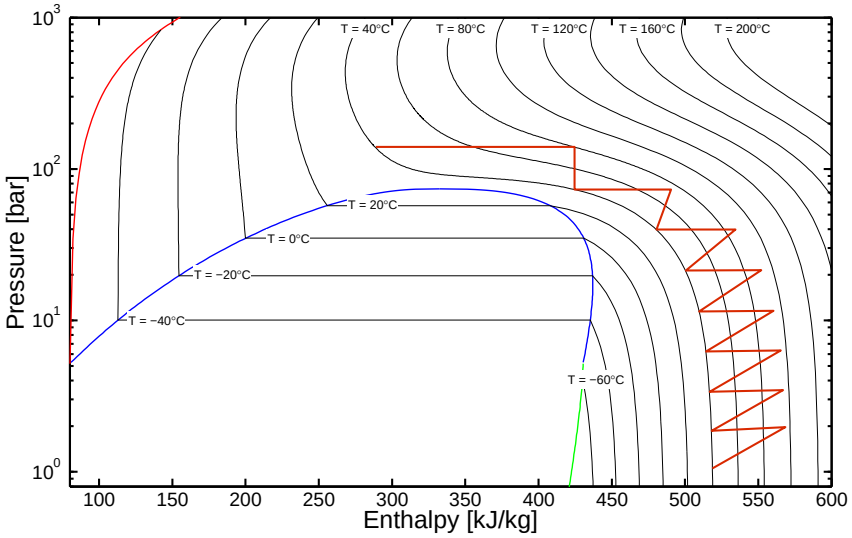

Figure 19: Straight compression process (dark red line) at the nominal state in pressure–enthalpy digram. Blue line is saturation line, light red is melting line and green is sublimation line.

liquid CO_2 pump was set to −33 °C even though CO_2 liquefies already at −27.5 °C in 15.5 bar pressure. Temperature was controlled with expansion valve in refrigerant cycle. Extra cooling makes it sure that CO_2 stays in liquid phase even during dynamic changes, this prevents cavitation of the pump.

Refrigerant ammonia cycle is a closed cycle. After the NH_3 has cooled the CO_2 stream, it is at low pressure. NH_3 need to be pressurized so that it can be liquidized with water cooling and then expanded with valve to low pressure and to low temperature. Number of compressor stages for NH_3 in the model is seven. The number of compressor stages was chosen similarly as in paper by Alabdulkarem et al. (2012). They mention that maximum outlet temperature from compressor stage is 90 °C for refrigerant to prevent excessive heat. NH_3 has temperature lines close to each other at superheated region, therefor seven compressor stages were used. Pressure ratio of the compressor stages was around 2. There was some divergence in pressure ratios as the outlet temperature of some compressor stages got too high. Pressure–enthalpy diagram for closed NH_3 cycle is shown in figure 20.

Pressure–enthalpy diagram of NH_3 in figure 20 shows that ammonia get overheated almost 60 °C before compression. Overheating is needed to prevent liquid refrigerant droplets to come into the compressor. Usually

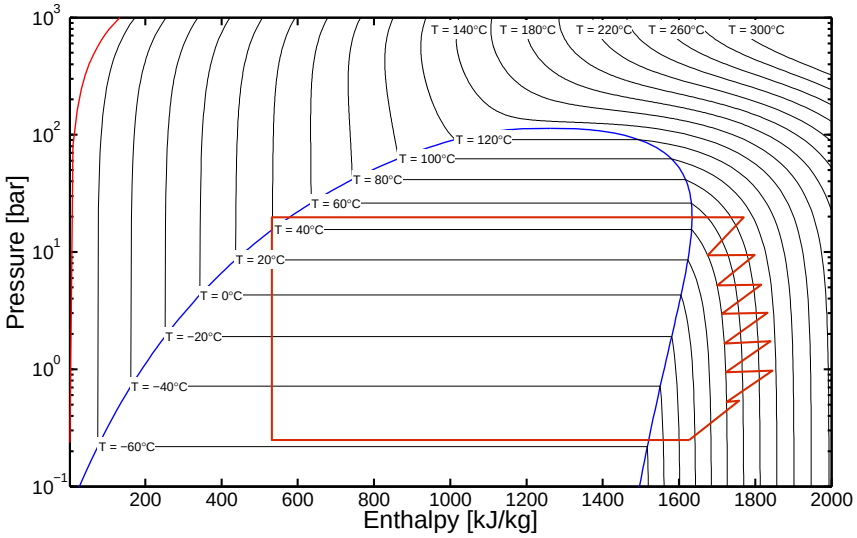

Figure 20: NH_3 cycle in compression liquid pumping model (dark red line) at the nominal state in pressure–enthalpy digram. Blue line is saturation line and light red is melting line.

overheating in refrigerant cycle is around 5 to 10 °C, 60 °C overheating is unnecessary high and causes only extra energy consumption. To prevent this the expansion valve control should be controlled based on the temperature at the refrigerant compression inlet. To this model it wasn't done because more concern was made to keep the CO_2 in liquid phase at CO_2 pump inlet.

Simplified process diagram for compression liquid pumping model is shown in figure 21. Compressor stages with water cooling for CO_2 and NH_3 are combined in to one compressor as they are similar to that shown in figure 18. For NH_3 cycle was needed a stabilizing side branch for calculations. Closed cycle is difficult for iterative calculations as it might find some unrealistic equilibrium or diverge easily. Side branch helps calculations as it gives possibility to lose or gain some mass flow if needed. Loosed or gained mass flow in simulations was really small and had no effect to the process. Leaking side branch effects also on the pressure levels of the NH_3 cycle. Side branch limits the maximum pressure after the NH_3 compression to the value used in the connection point at the of the side branch. Limit pressure used in the models with refrigerant cycle was 20 bars.

As there is no heat exchanger after the CO_2 pump, the CO_2 leaves the system at close to −33 °C temperature. Compression liquid pumping pro-

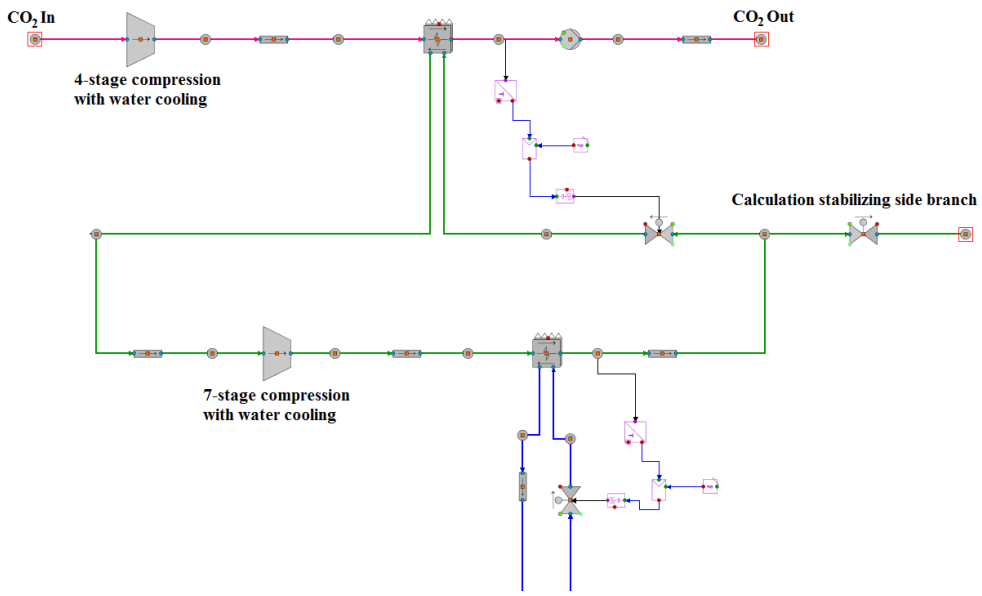

Figure 21: Simplified Apros diagram of the compression liquid pumping model. Red line is for CO_2, blue is cooling water and green is refrigerant NH_3.

cess is shown in pressure–enthalpy diagram in figure 22. By comparing figures 19 and 22 can be seen that with CO_2 in compression liquid pumping process is leaving significantly more cooling energy as for straight compression process. This cold energy should be used in the process to save energy. At the model below is shown one way to recover this cold energy from the liquid CO_2. This cold energy recovery has significant effect to the total energy consumption which is shown in section 6.1 at the table 9.

5.3.3 Compression liquid pumping with cold recovery

Main features of the model are similar as in previous model, but CO_2 is cycled back to subcool NH_3 stream after condenser and to precool the CO_2 stream before liquification. Simplified model diagram is shown in figure 23. Compared to model without cold recovery in figure 21 it can be seen that there is two extra heat exchangers in this model. Subcooled temperature for NH_3 was -10 °C instead of 40 °C. Precooling the CO_2 lowered its temperature to around 15 °C before liquification. After the last CO_2 compressor stage the temperature was around 98 °C.

Pressure–enthalpy digram of CO_2 for the process with cold recovery is shown in figure 24. Before leaving the process CO_2 has warmed up to

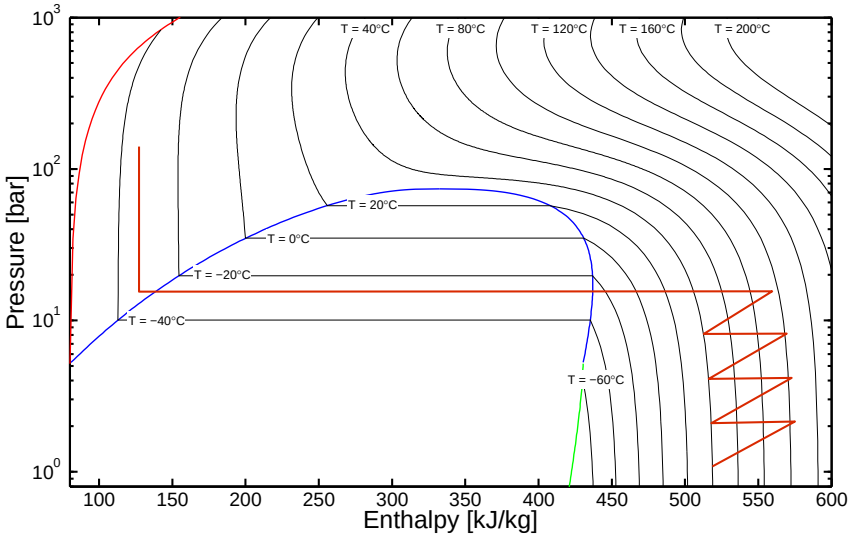

Figure 22: Compression liquid pumping process (dark red line) at the nominal state in pressure–enthalpy digram. Blue line is saturation line, light red is melting line and green is sublimation line.

34 °C. It could still be possible to get some more cold recovered with better heat exchanger design. This wasn't done as it was thought to have no significant effect to the process. Verification for this can be made by comparing the enthalpy differences between the CO_2 outlet points in figures 19 and 24.

Effect of the subcooling of the NH_3 can be seen in pressure–enthalpy digram of ammonia shown in figure 25. Ammonia subcools in liquid phase before the expansion valve drops its pressure to around 0.2 bar and temperature close to −60 °C. After the first compressor stage temperature of NH_3 is still below 40 °C and it is not cooled, but the pressure drop in the heat exchanger causes it to cool a bit. It is also possible to see that outlet temperatures of compressor stages 3 to 6 are over 90 °C. Some optimization should be done for the refrigerant cycle to prevent these high temperatures.

For some reason the cycle tends to go to maximum pressure determined by side branch even tough ammonia liquefies already at 15.5 bars at 40 °C temperature. Same problem was also with model without cold recovery. This unnecessarily high pressure causes unnecessary power consumption.

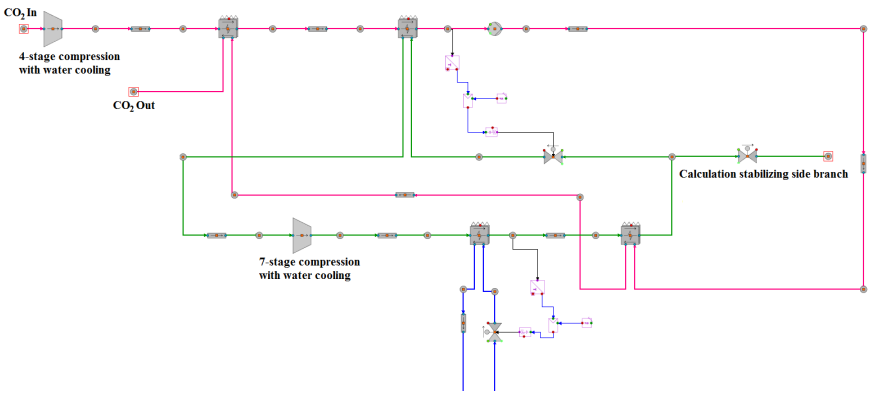

Figure 23: Simplified Apros diagram of the compression liquid pumping with cold recovery model. Red line is for CO_2, blue is cooling water and green is refrigerant NH_3.

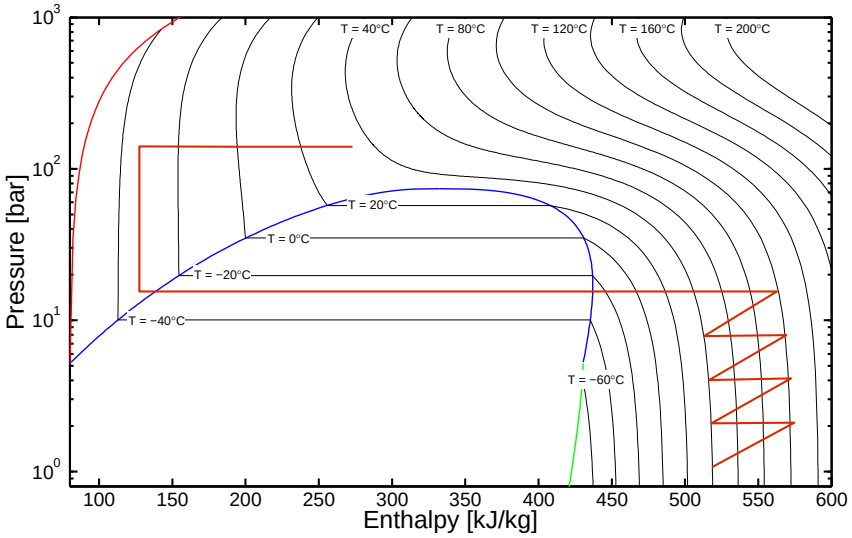

Figure 24: Compression liquid pumping with cold recovery process (dark red line) at the nominal state in pressure–enthalpy digram. Blue line is saturation line, light red is melting line and green is sublimation line.

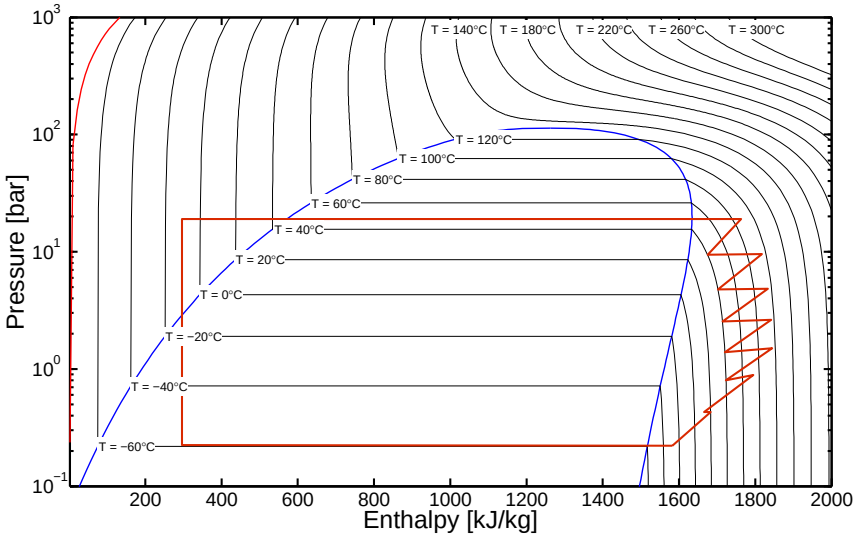

Figure 25: NH_3 cycle in compression liquid pumping with cold recovery model (dark red line) at the nominal state in pressure–enthalpy digram. Blue line is saturation line and light red is melting line.

6 SIMULATIONS AND RESULTS

At first models were verified with steady state simulations, as literature references were from steady state simulations. After the verifications, dynamic simulations were done. Changes to the model configurations were not made after the steady state simulations. Only changes in automations were made if needed, as steady state simulations don't fully test automations behavior.

6.1 Steady state simulations

For steady state result, models were simulated to equilibrium state until results were gathered. The nominal state of the models was used as the equilibrium state for steady state simulations. Comparison of the models was made mainly by comparing the total power consumptions. Total power consists all compressor stages powers (CO_2 and refrigerant), cooling water pump's total power and for models with liquid CO_2 pumping the CO_2 pump's power.

First straight compression model was validated against vendor's data for 8 stage compressor with similar mass flow and outlet pressure. Model fits to vendor's data relatively well as shown in table 8. Compressors have significant role in the total power consumption of the process as explained later in section 6.2. Due to this it is important to know that compressors are working realistically.

Table 8: Apros compressor validation against vendor's (Man Diesel & Turbo) data

	Apros model	Vendor's data
No. of stages	8	8
Mass flow [kg/s]	12	12
Inlet temperature [°C]	40	–
Inlet pressure [bar]	1.1	1.1
Outlet pressure [bar]	140	140
Polytropic efficiency [%]	80	–
Power [MW]	4.75	5

There is no information about the efficiency nor what is the inter cooled temperature before compressor stages for the vendor's compressor. For

this reason it is thought that the power consumption for the Apros model matches well enough with the vendor's data.

Straight compression is a conventional method for CO_2 pressurization for transportation and storing. Other modeled methods are attempt to find more energy efficient process for CO_2 liquidization. Comparison of the total power consumptions for the models at the nominal state are in table 9. In table 9 is also shown comparison between total power consumptions compared to straight compression model and power consumption comparison result by Alabdulkarem et al. (2012) for similar models.

Table 9: Total power consumption of different models, comparison of power consumptions to straight compression model and comparison results from similar models by Alabdulkarem et al. (2012).

	Total power [MW]	Comparison [%]	Reference results [%]
Straight compression	4.86	100	100
Compression liquid pumping	6.54	134.6	138.4
Compression liquid pumping w/ cold recovery	5.5	113.2	94.9

Table 9 shows that from these models straight compression method was the most energy efficient. But as can be seen from result by Alabdulkarem et al. (2012) that with compression liquid pumping with cold recovery can be more energy efficient. In their models Alabdulkarem et al. (2012) used different liquefaction pressures for CO_2 and result shown in table 9 is for 50 bar liquefaction pressure. Their result at 6 bar liquefaction pressure is 7.5 % less energy efficient than straight compression method. As the liquefaction pressure used in Apros models was 15.5 bars, results appear to be adequately close to ones by Alabdulkarem et al. (2012). With optimizing the liquefaction pressure it could be possible to get the model with cold recovery to be more energy efficient than straight compression model. Also getting the overheating temperature of refrigerant cycle to be smaller will increase efficiency of the processes with refrigerant cycle.

In literature (Alabdulkarem et al., 2012, Aspelund and Jordal, 2007, Romeo et al., 2009) is said that CO_2 liquidization consumes typically from 90 to 120 kWh/ton CO_2. For comparison straight compression modeled in this thesis consumes 112.5 kWh/ton CO_2 and most inefficient compression with liquid pumping consumes 151 kWh/ton CO_2. It

can be said that results got from these simulations are at the upper end of the typical consumption scale.

6.2 Dynamic simulations

Dynamic behavior of the models was tested with two different step change test. First test was with the CO_2 mass flow set point and another with cooling water temperature. In table 10 is shown step changes and their orderings. Between the changes simulations were running until new equilibrium state was reached.

Table 10: Step change parameters and values made with the models. After a change the process was simulated until stabilization before new change.

Parameter	Value
CO_2 mass flow set point [kg/s]	6
CO_2 mass flow set point [kg/s]	12
CO_2 mass flow set point [kg/s]	9
CO_2 mass flow set point [kg/s]	12
Cooling water temperature [°C]	20
Cooling water temperature [°C]	35
Cooling water temperature [°C]	30
Cooling water temperature [°C]	35

Before the results were gathered, process controls were tested with various step change tests. PI controllers gain and integration time values were altered if there was some unwanted behavior happening in the models. As a rule of thumb was that controls for temperature has long integration time and controls for mass flow and pressure are reacting faster.

For models with liquid CO_2 pumping, it was checked that CO_2 stays in liquid phase before the pump during all tests. At first step change in CO_2 mass flow caused vapor formation before the pump. It was noticed that CO_2 compressors reacted much faster to the change than the liquid CO_2 pump and refrigerant cycle valve. To prevent this the step change was ramped to the compressor stages with gradient of $1\frac{1}{min}$. This slowed change in CO_2 compressors enough that pressure and temperature before the pump stayed within acceptable limits.

6.3 Effect of CO_2 mass flow changes

After the controls were tuned up and running, it was possible to start dynamic step change simulations. Simulations started from nominal state. In figure 26 is shown result how changes in CO_2 mass flow affects to the total power consumption of the processes.

From figure 26 can be seen that as the model gets more complicated it reacts slower to the changes. Controls are working well as there are no oscillations or other fluctuations in total power. Total power is dominated by compressor powers as halving the CO_2 mass flow more or less halves the total power.

For straight compression model the total power consumption goes even below half when halving the CO_2 mass flow. This is due to the fact that with smaller mass flow there is less pressure losses in heat exchangers and pipes, and this causes to compressor stages to have smaller pressure ratios. Smaller pressure ratio means smaller power consumption in compressors (equation (5)). In reality compressor power consumption probably shouldn't get halved, because the polytropic efficiency of the compressor should decrease with undesigned mass flows (see figure 6). Apros models are not taking this into account as mentioned earlier.

For models with refrigerant cycle the total power consumptions are staying a bit above the half when CO_2 mass flow is halved. In these models the NH_3 compressor stages are having higher pressure ratios with smaller mass flow. Increase in pressure ratios increases the total power consumption. Reason for higher pressure ratios was uncontrollable pressure levels in refrigerant cycle. When CO_2 mass flow was altering the NH_3 mass flow changed also. Even though refrigerant cycle was closed iterative calculations can change the mass flow in the cycle. But this can be thought to be caused by equalizing tank in the cycle. Calculation stabilizing side branch was not affecting to the mass flow more than some fractions. With lower mass flow of NH_3 the refrigerant expansion got further to lower pressure and temperature levels. Lower pressure level after the expansion valve causes the overall pressure ratio in refrigerant cycle to be higher as the high pressure is not decreasing.

One reason for pressure level behavior was non optimal control logics. In these models the only control for refrigerant cycle was at the expansion

valve. Expansion valve was controlled by the temperature in CO_2 line, which might cause the problems. Maybe better control measurement for expansion valve could be the temperature after the CO_2 heat exchanger. This method could limit the overheating also closer to typical overheating temperature.

Effect of CO_2 mass flow change can be better seen if total power consumptions are turned to specific work values. In table 11 is shown what effect the mass flow has to the specific work.

Table 11: Specific works for different models with different CO_2 mass flows.

CO_2 mass flow [kg/s]	12	9	6
Straight compression [kJ/kg]	405	400	398
Compression liquid pumping [kJ/kg]	545	556	567
Compression liquid pumping w/ cold recovery [kJ/kg]	458	466	480

Specific work for straight compression model was quite constant through the CO_2 mass flow change tests, as can be seen from table 11. Small changes in specific work can be explained by the decrease in pressure losses as described earlier. For other models the changes in specific work are higher. High changes can only be explained by changes in compressor properties, as compressors have the highest effect to the total power consumption. Only pressure ratio changes in refrigerant cycle are capable to explain these changes in specific work values shown in table 11. Also the fact that specific work was decreasing in straight compression model as mass flow decreases, but increases in other two models indicates that explanation is in the refrigerant cycle.

6.4 Effect of cooling water temperature changes

After the CO_2 mass flow step change simulations were done the models were set back to nominal equilibrium state. The cooling water step change experiments shown in table 10 were started from nominal state. Again before next step change the model was waited to reach equilibrium state. Results for all the models are shown in figure 27. As mentioned above, the inlet temperature for compressor stages (CO_2 and NH_3) were 5 °higher than the cooling water temperature. This means that with cooling water temperature of 20 °C the temperatures before compressor stages were 25 °C. Exception to this was the temperature before straight

compression model's last compressor stage. There pressure was already above the CO_2 critical point, which means that CO_2 turns to liquid at temperatures below 31 °C. To prevent liquid formation before the last compressor stage, the temperature was limited to 35 °C.

For these simulations the control settings were the same as in CO_2 mass flow change simulations. From figure 27 can be seen that these control setting were not optimal for cooling water temperature changes as there is quite high fluctuations in total power consumptions. Sudden drop on inlet temperature to compressor stage causes the mass flow through compressor to jump up. Compressor stages rotation speed is too high compared to the quality of the inlet fluid. Rotational speeds were changing slower than the temperature in fluids before compressor stages. Cooler fluid is denser than warmer and it was possible to get more fluid through the compressor stages. As mentioned, compressor power consumption is directly proportional to the mass flow and higher mass flow results to higher power consumptions. Of course in changes to warmer cooling water temperatures the situation is the opposite.

Again highest effect to the total power consumption was the compressor power consumptions. Compressor power consumption is directly proportional to the inlet temperature (equation (5)), but in Kelvin scale. Thus the total powers were not dropping to almost half as the temperature drops to almost half in Celsius scale. Total power consumptions turned to specific works are shown in table 12. In these simulations CO_2 mass flow was kept on 12 kg/s. Specific work gets smaller as cooling water gets colder. This is an outcome from the fact that CO_2 is denser and volume flow is smaller, even though mass flow is the same, smaller volume flow in compressors means smaller power consumption. On pressure-enthalpy diagram compression path gets closer to the saturation line.

Table 12: Total power consumptions for different models with different cooling water temperatures.

Cooling water temperature [°C]	35	30	20
Straight compression [kJ/kg]	405	398	386
Compression liquid pumping [kJ/kg]	545	527	497
Compression liquid pumping w/ cold recovery [kJ/kg]	458	450	433

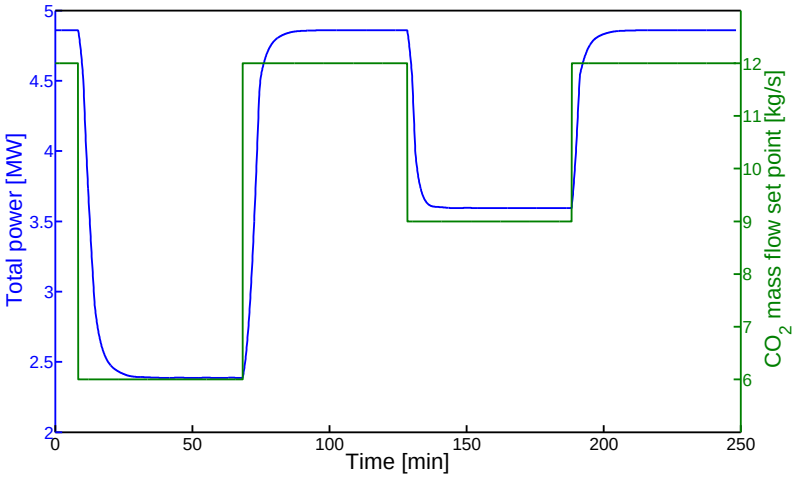

(a) Straight compression

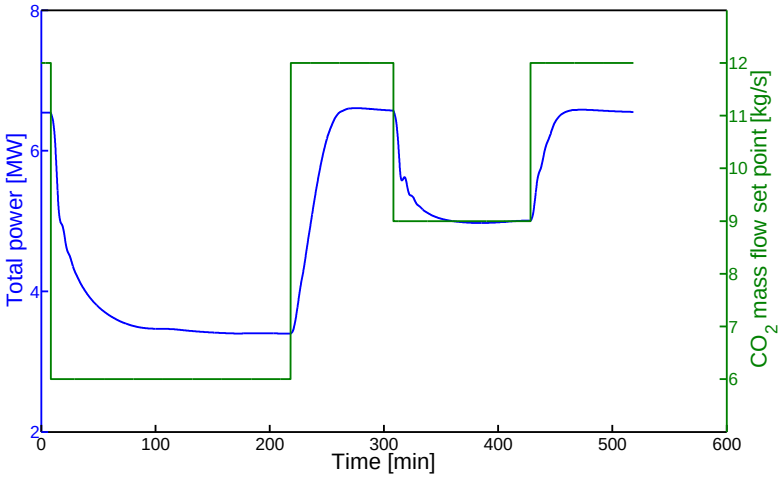

(b) Compression liquid pumping

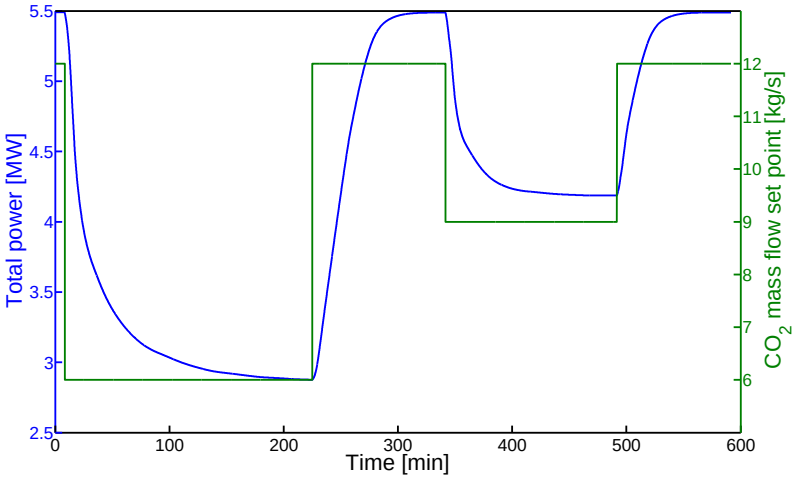

(c) Compression liquid pumping with cold recovery

Figure 26: Effect of CO_2 mass flow set point changes to total power consumption in different models.

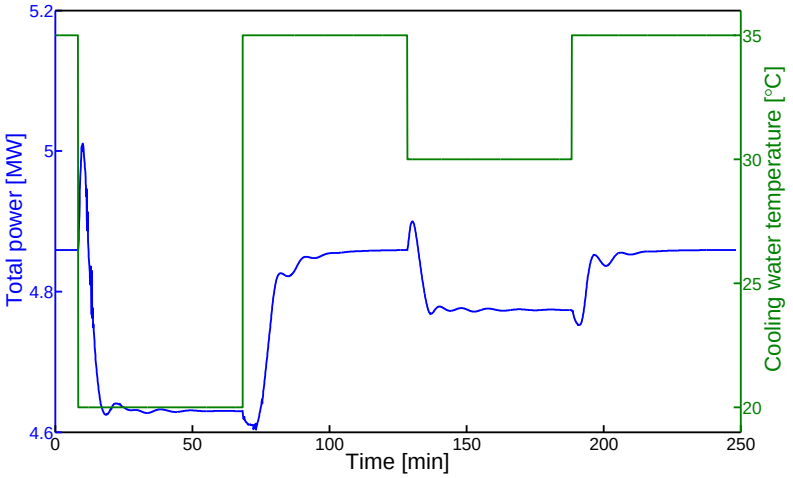

(a) Straight compression

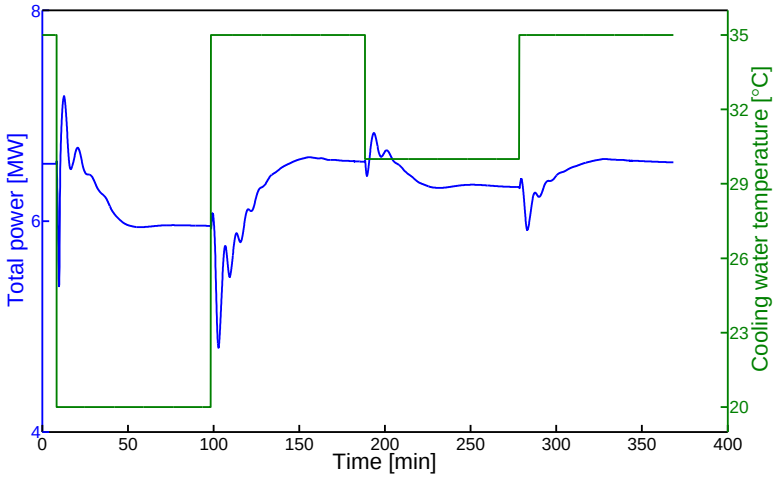

(b) Compression liquid pumping

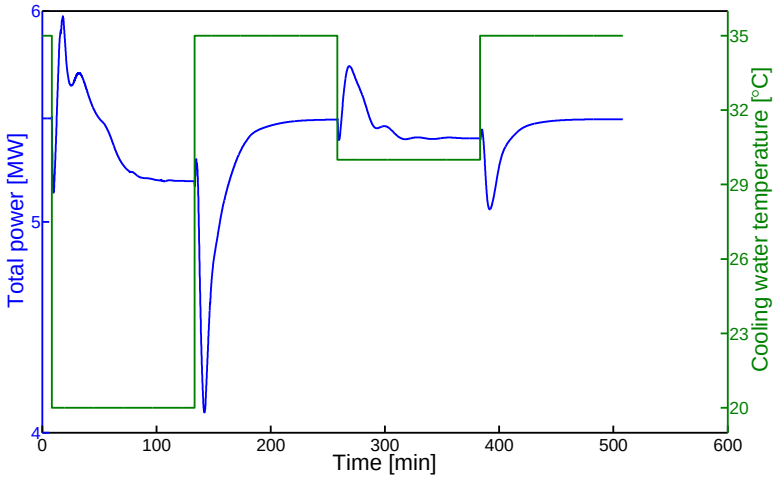

(c) Compression liquid pumping with cold recovery

Figure 27: Effect of cooling water temperature changes to total power consumption in different models.

7 CONCLUSION

In this thesis the process of CO_2 liquidization was studied. First a literature review of the process was made. Literature review consists the theory for CO_2 liquidization and compression, transportation and storing of pressurized CO_2. Also some processes in which CO_2 can be used was presented. Main focus on the reviews of transportation, storing and utilization processes was temperature, pressure and purity levels, as they are most important things concerning the liquidization process.

Theoretical part of the thesis was development of three dynamic models of CO_2 liuidization process. Models made were straight compression model, and two compression liquid pumping models: one with and one without cold energy recovery. Models were made with Apros 6 Combustion process simulation software. Apros model components accuracy against reality was tested with the straight compression model. Accuracy was found to be sufficient, as all vendor's measurement configurations were not informed.

Dynamic behavior of the models was tested with two different step change tests. In the first test the CO_2 mass flow changed and on the second test cooling water temperature changed. At the mass flow step change tests all tree models worked well and no fluctuations during transients was noticed. In cooling water step change tests all three models suffered from fluctuations. Better behavior in mass flow change tests can be explained with the fact that step changes effect was a bit ramped while cooling water temperature change was instant.

More development should be made on the models with refrigerant cooling cycle. Pressure level controlling in closed cycle was difficult and caused some unfavorable results. One was over pressurizing the refrigerant before the expansion valve and expanding to unnecessary low pressure. This causes unnecessary power consumption and makes these models less efficient. Partly for this reason the straight compression model was found most efficient, even though in literature compression liquid pumping model with cold recovery have been found at least as efficient in literature. Controllability of refrigerant cycle could be increased with better control logic. Also optimization on CO_2 condensing pressure could be made, as it might be possible to find more efficient pressure level than

15.5 bars used in this thesis.

In future these models could be modified to work with mixture fluids. Upcoming Apros update should provide possibility to use mixtures. Modifications are needed as there aren't any purification equipment implemented to these models. At least water could be included to the CO_2 stream and water separation columns between compressor stages.

Another possible future study could be refrigerant cycle models with other refrigerants. Other refrigerants could be more efficient than the NH_3 used in the models now. Other refrigerants could need less compressor stages which could lead to smaller power consumption for the process. Also simpler refrigerant cycle might be easier to handle.

Automations of the models should be modified if combined with models of other processes. For example if model of CO_2 capture process is combined to models presented in this theses, should CO_2 mass flow be controlled other way. Now compressor stages are compressing constant mass flow, but capture process might provide CO_2 in fluctuating manner. When CO_2 flow from capture process is smaller than what compressor stages are trying to achieve, this could cause negative pressure before compressor stages. Negative pressure could effect negatively to capture and compression processes. One way to prevent this could be that compressor stages are controlled by the pressure levels before and after them. This way there shouldn't be able to become unwanted pressure levels in to the system.

REFERENCES

Air Compressor Works, Inc. [In Air Compressor Works, Inc. www-pages], 2015. URL http://www.aircompressorworks.com/blog/index.php?mode=post&id=27. [retrieved February 19, 2015].

Alabdulkarem, A., Hwang, Y., and Radermacher, R. Development of CO_2 liquefaction cycles for CO_2 sequestration. *Applied Thermal Engineering*, 33–34(0):144 – 156, 2012. ISSN 1359-4311. doi: http://dx.doi.org/10.1016/j.applthermaleng.2011.09.027. URL http://www.sciencedirect.com/science/article/pii/S1359431111005114.

Amrollahi, Z., Ertesvåg, I. S., and Bolland, O. Thermodynamic analysis on post-combustion CO_2 capture of natural-gas-fired power plant. *International Journal of Greenhouse Gas Control*, 5(3):422 – 426, 2011. ISSN 1750-5836. doi: http://dx.doi.org/10.1016/j.ijggc.2010.09.004. URL http://www.sciencedirect.com/science/article/pii/S1750583610001428. The 5thTrondheim Conference on CO_2 Capture, Transport and Storage.

Apros User Manual. 2014.

Apros web page, 2014. URL http://www.apros.fi.

Aresta, M. and Dibenedetto, A. Utilisation of co2 as a chemical feedstock: opportunities and challenges. *Dalton Trans.*, pages 2975–2992, 2007. doi: 10.1039/B700658F. URL http://dx.doi.org/10.1039/B700658F.

Asia Vacuum Pumps. [In Asia Vacuum Pumps www-pages], 2015. URL http://asiavacuumpumps.com/Comperssor. [retrieved February 19, 2015].

Aspelund, A., Mølnvik, M., and Koeijer, G. D. Ship transport of co2: Technical solutions and analysis of costs, energy utilization, exergy efficiency and CO_2 emissions. *Chemical Engineering Research and Design*, 84(9):847 – 855, 2006. ISSN 0263-8762. doi: http://dx.doi.org/10.1205/cherd.5147. URL http://www.sciencedirect.com/science/article/pii/S0263876206729665.

Aspelund, A. and Jordal, K. Gas conditioning—the interface between CO_2 capture and transport. *International Journal of Greenhouse Gas*

Control, 1(3):343 – 354, 2007. ISSN 1750-5836. doi: http://dx.doi.org/10.1016/S1750-5836(07)00040-0. URL http://www.sciencedirect.com/science/article/pii/S1750583607000400.

Bilsbak, V. Conditioning of CO_2 coming from a CO_2 capture process for transport and storage purposes. Master's thesis, Norwegian University of Science and Technology, 2009.

Bui, M., Gunawan, I., Verheyen, V., Feron, P., Meuleman, E., and Adeloju, S. Dynamic modelling and optimisation of flexible operation in post-combustion CO_2 capture plants—a review. *Computers & Chemical Engineering*, 61(0):245 – 265, 2014. ISSN 0098-1354. doi: http://dx.doi.org/10.1016/j.compchemeng.2013.11.015. URL http://www.sciencedirect.com/science/article/pii/S0098135413003669.

Celica Tech. [In Celica Tech forum www-pages], 2015. URL http://emspowered.com/images/products/turbokit/compressormaps/S250_compressor_map.jpg. [retrieved February 19, 2015].

Chapoy, A., Nazeri, M., Kapateh, M., Burgass, R., Coquelet, C., and Tohidi, B. Effect of impurities on thermophysical properties and phase behaviour of a CO_2-rich system in ccs. *International Journal of Greenhouse Gas Control*, 19(0):92 – 100, 2013. ISSN 1750-5836. doi: http://dx.doi.org/10.1016/j.ijggc.2013.08.019. URL http://www.sciencedirect.com/science/article/pii/S1750583613003186.

Cifre, P. G., Brechtel, K., Hoch, S., García, H., Asprion, N., Hasse, H., and Scheffknecht, G. Integration of a chemical process model in a power plant modelling tool for the simulation of an amine based CO_2 scrubber. *Fuel*, 88(12):2481 – 2488, 2009. ISSN 0016-2361. doi: http://dx.doi.org/10.1016/j.fuel.2009.01.031. URL http://www.sciencedirect.com/science/article/pii/S0016236109000490. 7th European Conference on Coal Research and Its Applications.

CSLF. Carbon sequestration leadership forum technology roadmap 2013. Technical report, 2013.

Duan, L., Chen, X., and Yang, Y. Study on a novel process for CO_2 compression and liquefaction integrated with the refrigeration process. *International Journal of Energy Research*, 37(12):1453–1464, 2013.

ISSN 1099-114X. doi: 10.1002/er.2951. URL http://dx.doi.org/10.1002/er.2951.

ENCAP. Power systems evaluation and benchmarking, 2008. URL http://www.encapco2.org/publications/D_1_2_4_summaryReport.pdf.

Forbes, S., Verma, P., Curry, T. E., Bradley, M., LLC, A., Friedmann, D. S. J., Laboratory, L. L. N., and Wade, S. M. *CCS Guidelines: Guidelines for Carbon Dioxide Capture, Transport, and Storage*. World Resources Institute (WRI), Washington, DC: WRI, 2008. ISBN 978-1-56973-701-9.

Friedmann, S. J. Energy: A geoscience perspective: Geological carbon dioxide sequestration. *Elements*, 3:179 – 184, 2007. doi: 10.2113/gselements.3.3.179.

Fu, C. and Gundersen, T. Carbon capture and storage in the power industry: Challenges and opportunities. *Energy Procedia*, 16, Part C (0):1806 – 1812, 2012. ISSN 1876-6102. doi: http://dx.doi.org/10.1016/j.egypro.2012.01.278. URL http://www.sciencedirect.com/science/article/pii/S1876610212002883. 2012 International Conference on Future Energy, Environment, and Materials.

Gao, J., Wang, Y., Ping, Y., Hu, D., Xu, G., Gu, F., and Su, F. A thermodynamic analysis of methanation reactions of carbon oxides for the production of synthetic natural gas. *RSC Adv.*, 2:2358–2368, 2012. doi: 10.1039/C2RA00632D. URL http://dx.doi.org/10.1039/C2RA00632D.

Gibbins, J. and Chalmers, H. Carbon capture and storage. *Energy Policy*, 36(12):4317 – 4322, 2008. ISSN 0301-4215. doi: http://dx.doi.org/10.1016/j.enpol.2008.09.058. URL http://www.sciencedirect.com/science/article/pii/S0301421508004436. Foresight Sustainable Energy Management and the Built Environment Project.

Göttlicher, G. *The Energetics of Carbon Dioxide Capture in Power Plants*. U . S . Depar tment of Energy, 2004.

Herzog, H. J. Scaling up carbon dioxide capture and storage: From megatons to gigatons. *Energy Economics*, 33(4):597 – 604, 2011. ISSN 0140-9883. doi: http://dx.doi.org/10.1016/j.eneco.2010.11.004. URL http://www.sciencedirect.com/science/article/pii/

S0140988310001921. Special Issue on The Economics of Technologies to Combat Global Warming.

Hill, B., Hovorka, S., and Melzer, S. Geologic carbon storage through enhanced oil recovery. *Energy Procedia*, 37(0):6808 – 6830, 2013. ISSN 1876-6102. doi: http://dx.doi.org/10.1016/j.egypro.2013.06.614. URL http://www.sciencedirect.com/science/article/pii/S1876610213008576. GHGT-11.

Hill, P. G. P. G. and Peterson, C. R. *Mechanics and thermodynamics of propulsion*. Reading, Mass. : Addison-Wesley Pub. Co, 1965.

Hänninen, M. and Ylijoki, J. The one-dimensional separate two-phase flow model of apros, 2008. ISSN 1455-0865. URL http://www.vtt.fi/inf/pdf/tiedotteet/2008/T2443.pdf.

Holloway, S. Storage of fossil fuel-derived carbon dioxide beneath the surface of the earth. *Annual Review of Energy & the Environment*, 26 (1):145, 2001. ISSN 10563466. URL http://search.ebscohost.com/login.aspx?direct=true&db=asr&AN=6533473&site=ehost-live.

Hwang, S., Lee, J., Hong, U. G., Seo, J. G., Jung, J. C., Koh, D. J., Lim, H., Byun, C., and Song, I. K. Methane production from carbon monoxide and hydrogen over nickel–alumina xerogel catalyst: Effect of nickel content. *Journal of Industrial and Engineering Chemistry*, 17 (1):154 – 157, 2011. ISSN 1226-086X. doi: http://dx.doi.org/10.1016/j.jiec.2010.12.015. URL http://www.sciencedirect.com/science/article/pii/S1226086X10002911.

IEA. Greenhouse gas r&d programme, "capturing CO_2,". 2007. URL http://www.ieaghg.org/docs/general_publications/cocapture.pdf.

IEC. Electrical energy storage. Technical report, 2011. International Electrotechnical Commission.

IPCC. *Special Report on Carbon Dioxide Capture and Storage*. Cambridge University Press, Cambridge, United Kingdom and New York, NY, USA, 2005. Presented by Working Group III of the Intergovernmental Panel on Climate Change [Metz, B., O. Davidson, H. C. de Coninck, M. Loos, and L. A. Meyer (eds.)].

IPCC. *Climate Change 2007: Mitigation. Contribution of Working*

Group III to the Fourth Assessment Report of the Intergovernmental Panel on Climate Change. Cambridge University Press, Cambridge, United Kingdom and New York, NY, USA, 2007. [B. Metz, O.R. Davidson, P.R. Bosch, R. Dave, L.A. Meyer (eds)].

Kohl, A. L. and Nielsen, R. B. Chapter 12 - gas dehydration and purification by adsorption. In Kohl, A. L. and Nielsen, R. B., editors, *Gas Purification (Fifth Edition)*, pages 1022 – 1135. Gulf Professional Publishing, Houston, fifth edition edition, 1997a. ISBN 978-0-88415-220-0. doi: http://dx.doi.org/10.1016/B978-088415220-0/50012-4. URL http://www.sciencedirect.com/science/article/pii/B9780884152200500124.

Kohl, A. L. and Nielsen, R. B. Chapter 7 - sulfur dioxide removal. In Kohl, A. L. and Nielsen, R. B., editors, *Gas Purification (Fifth Edition)*, pages 466 – 669. Gulf Professional Publishing, Houston, fifth edition edition, 1997b. ISBN 978-0-88415-220-0. doi: http://dx.doi.org/10.1016/B978-088415220-0/50007-0. URL http://www.sciencedirect.com/science/article/pii/B9780884152200500070.

Kvamsdal, H. M., Jordal, K., and Bolland, O. A quantitative comparison of gas turbine cycles with CO_2 capture. *Energy*, 32(1):10 – 24, 2007. ISSN 0360-5442. doi: http://dx.doi.org/10.1016/j.energy.2006.02.006. URL http://www.sciencedirect.com/science/article/pii/S036054420600048X.

Lüdtke, K. H. *Process Centrifugal Compressors: Basics, Function, Operation, Design, Application*. Springer Berlin Heidelberg, Berlin, Heidelberg, 2004. ISBN 9783642073304; 9783662094495; 3662094495; 3642073301.

Le Quéré, C., Moriarty, R., Andrew, R. M., and et al. Global carbon budget 2014. *Earth System Science Data Discussions*, 7(2): 521–610, 2014. doi: 10.5194/essdd-7-521-2014. URL http://www.earth-syst-sci-data-discuss.net/7/521/2014/.

Lee, U., Lim, Y., Lee, S., Jung, J., and Han, C. CO_2 storage terminal for ship transportation. *Industrial & Engineering Chemistry Research*, 51(1):389–397, 2012. doi: 10.1021/ie200762f. URL http://dx.doi.org/10.1021/ie200762f.

Leung, D. Y., Caramanna, G., and Maroto-Valer, M. M. An overview of current status of carbon dioxide capture and storage technologies. *Renewable and Sustainable Energy Reviews*, 39(0):426 – 443, 2014. ISSN 1364-0321. doi: http://dx.doi.org/10.1016/j.rser.2014.07.093. URL http://www.sciencedirect.com/science/article/pii/S1364032114005450.

Man Diesel & Turbo. Forward thinking, advanced CO_2 compression solutions. URL http://www.mandiesel.com.cn/files/news/filesof12086/CO2_ForwardThinking_li4_lowres.pdf.

Maramba, T. and Bhattacharya, D. CO_2 compression and dehydration for carbon capture and sequestration. 2011. URL http://www.bechtel.com/assets/files/TechJournal/2011/OG&C%2004%20CO2%20Compression%20Final.pdf.

Meyer, J. P. Summary of carbon dioxide enhanced oil recovery (CO_2 EOR) injection well technology. Technical report, 2007. American Petroleum Institute.

Möller, B. F., Genrup, M., and Assadi, M. On the off-design of a natural gas-fired combined cycle with CO_2 capture. *Energy*, 32(4):353 – 359, 2007. ISSN 0360-5442. doi: http://dx.doi.org/10.1016/j.energy.2006.07.022. URL http://www.sciencedirect.com/science/article/pii/S0360544206002210. {ECOS} 05. 18th International Conference on Efficiency, Cost, Optimization, Simulation, and Environmental Impact of Energy Systems {ECOS} 05.

Moore, J. J., Nored, M. G., Gernentz, R. S., and Brun, K. *Novel Concepts for the Compression of Large Volumes of Carbon Dioxide*. Sep 2007. doi: 10.2172/918688. URL http://www.osti.gov/scitech/servlets/purl/918688.

NETL, 2014. URL http://www.netl.doe.gov/research/coal/carbon-storage/research-and-development/co2-utilization.

Peebles, D. E., Goodman, D. W., and White, J. M. Methanation of carbon dioxide on nickel(100) and the effects of surface modifiers. *The Journal of Physical Chemistry*, 87(22):4378–4387, 1983. doi: 10.1021/j100245a014. URL http://dx.doi.org/10.1021/j100245a014.

Pfaff, I., Oexmann, J., and Kather, A. Optimised integration of post-

combustion CO_2 capture process in greenfield power plants. *Energy*, 35(10):4030 – 4041, 2010. ISSN 0360-5442. doi: http://dx.doi.org/10.1016/j.energy.2010.06.004. URL http://www.sciencedirect.com/science/article/pii/S036054421000318X.

Ramgen Power Systems. CO_2 compressor, 2014. Available from: http://www.ramgen.com/apps_comp_unique.html.

Ravagnani, A. G., Ligero, E., and Suslick, S. CO_2 sequestration through enhanced oil recovery in a mature oil field. *Journal of Petroleum Science and Engineering*, 65(3–4):129 – 138, 2009. ISSN 0920-4105. doi: http://dx.doi.org/10.1016/j.petrol.2008.12.015. URL http://www.sciencedirect.com/science/article/pii/S0920410509000072.

Romeo, L. M., Bolea, I., Lara, Y., and Escosa, J. M. Optimization of intercooling compression in CO_2 capture systems. *Applied Thermal Engineering*, 29(8–9):1744 – 1751, 2009. ISSN 1359-4311. doi: http://dx.doi.org/10.1016/j.applthermaleng.2008.08.010. URL http://www.sciencedirect.com/science/article/pii/S135943110800344X.

Sanpasertparnich, T., Idem, R., Bolea, I., deMontigny, D., and Tontiwachwuthikul, P. Integration of post-combustion capture and storage into a pulverized coal-fired power plant. *International Journal of Greenhouse Gas Control*, 4(3):499 – 510, 2010. ISSN 1750-5836. doi: http://dx.doi.org/10.1016/j.ijggc.2009.12.005. URL http://www.sciencedirect.com/science/article/pii/S1750583609001650.

Svensson, R., Odenberger, M., Johnsson, F., and Strömberg, L. Transportation systems for CO_2—application to carbon capture and storage. *Energy Conversion and Management*, 45(15–16):2343 – 2353, 2004. ISSN 0196-8904. doi: http://dx.doi.org/10.1016/j.enconman.2003.11.022. URL http://www.sciencedirect.com/science/article/pii/S0196890403003662.

Vermeulen, T. N. Knowledge sharing report – CO_2 liquid logistics shipping concept (llsc) overall supply chain optimization. Technical report, 2011. Global CCS Institute.

Wall, T. F. Combustion processes for carbon capture. *Proceedings of the Combustion Institute*, 31(1):31 – 47, 2007. ISSN 1540-7489. doi: http://dx.doi.org/10.1016/j.proci.2006.08.123. URL http://www.sciencedirect.com/science/article/pii/S1540748906003865.

Wei, W. and Jinlong, G. Methanation of carbon dioxide: an overview. *Frontiers of Chemical Science and Engineering*, 5(1):2–10, 2011. ISSN 2095-0179. doi: 10.1007/s11705-010-0528-3. URL http://dx.doi.org/10.1007/s11705-010-0528-3.

Xu, G., Liang, F., Yang, Y., Hu, Y., Zhang, K., and Liu, W. An improved co2 separation and purification system based on cryogenic separation and distillation theory. *Energies*, 7(5):3484–3502, 2014. ISSN 1996-1073. doi: 10.3390/en7053484. URL http://www.mdpi.com/1996-1073/7/5/3484.

Yin, X. Recovery and chemical utilization of carbon dioxide from fossil fuel burning industrial sources. *Journal of Environmental Sciences.*, pages 129–137, 1995. ISSN 1001-0742.

Zanganeh, K. E. and Shafeen, A. A novel process integration, optimization and design approach for large-scale implementation of oxy-fired coal power plants with CO_2 capture. *International Journal of Greenhouse Gas Control*, 1(1):47 – 54, 2007. ISSN 1750-5836. doi: http://dx.doi.org/10.1016/S1750-5836(07)00035-7. URL http://www.sciencedirect.com/science/article/pii/S1750583607000357. 8th International Conference on Greenhouse Gas Control Technologies GHGT-8.

Zhang, Z., Wang, G., Massarotto, P., and Rudolph, V. Optimization of pipeline transport for CO_2 sequestration. *Energy Conversion and Management*, 47(6):702 – 715, 2006. ISSN 0196-8904. doi: http://dx.doi.org/10.1016/j.enconman.2005.06.001. URL http://www.sciencedirect.com/science/article/pii/S0196890405001561.